Generation and characterization of vestibular inner ear organoids from human pluripotent stem cells

Valk, W.H. van der; Nist-Lund, C.; Zhang, J.Y.; Perea, C.; Jin, J.H.; Gim, K.Y.; ... ; Koehler, K.R.

nature protocols

https://doi.org/10.1038/s41596-025-01191-3

Protocol extension

Check for updates

Generation and characterization of vestibular inner ear organoids from human pluripotent stem cells

Wouter H. van der Valk[1,2,3,4,5,9], Carl Nist-Lund[1,2,3,9], Jingyuan Zhang[1,2,3,9], Camila Perea[1,2], Jiahe Jin[1,2], Kelly Y. Gim[1,2], Matthew R. Steinhart[1,6,7], Jiyoon Lee[1,2,3,8] ✉ & Karl R. Koehler[1,2,3,6,8] ✉

Abstract

The inner ear has a pivotal role in auditory and vestibular perception. Despite the vast number of individuals worldwide affected by hearing loss and balance disorders, therapeutic options have been largely limited to technological aids. The recent advent of gene therapies for genetic hearing loss in human patients underscores the urgency of developing scalable platforms to investigate a broader spectrum of inner ear disorders. Although animal models are powerful for assessing auditory and vestibular dysfunction, in vitro human inner ear models have shown promise in disease modeling and as platforms for studying developmental biology. Several studies have demonstrated that stem cells can be guided to differentiate into otic progenitor cells by mimicking environmental cues present during normal fetal inner ear development. Here we present a step-by-step approach to creating inner ear organoids (IEOs), which is an extension of our previous method for skin organoid generation, with which it shares foundational methodology and reagents. We used these organoids to elucidate the subtle signaling cues that govern their developmental trajectories. Generating sensory hair cells takes about 40 d, and cultures can be maintained for up to 150 d to allow further development. Moreover, we outline methods for assessing late-stage organoids, including whole-mount imaging of cleared IEOs, vibratome sectioning of live and fixed IEOs and other endpoint analyses, to study inner ear biology. IEOs are ideal for investigating human inner ear development, studying the mechanisms of inner ear disorders and developing therapeutic strategies. This protocol requires proficiency in basic stem cell culture techniques.

This protocol is an extension to: *Nat. Protoc.* **17**, 1266–1305 (2022): https://doi.org/10.1038/s41596-022-00681-y

Key points

- This is a protocol for the generation and characterization of vestibular inner ear organoids from human pluripotent stem cells. This is an extension of a previous protocol for skin organoid generation, with which it shares foundational methodology and reagents.
- Using a human-based system enables the modelling of features of human vestibular and auditory function, including several features that cannot be recapitulated using animal models.

Key references

Lee, J. et al. *Nat. Protoc.* **17**, 1266-1305 (2022): https://doi.org/10.1038/s41596-022-00681-y

Koehler, K. R. et al. *Nat. Biotechnol.* **35**, 583–589 (2017): https://doi.org/10.1038/nbt.3840

van der Valk, W. H. et al. *Cell Rep.* **42**, 112623 (2023): https://doi.org/10.1016/j.celrep.2023.112623

Steinhart, M. R. et al. *Development* **150**, dev201871 (2023): https://doi.org/10.1242/dev.201871

A full list of affiliations appears at the end of the paper. ✉e-mail: jiyoon.lee@childrens.harvard.edu; karl.koehler@childrens.harvard.edu

Introduction

The inner ear is a complex organ that contains sensory detectors known as hair cells, which are responsible for hearing, head tilt and orientation and both rotational and linear acceleration/deceleration (Fig. 1). These hair cells are extremely delicate and susceptible to a host of pathological traumas, such as genetic mutation, acoustic or vibrational blast trauma, small molecule ototoxicity or viral infection, all of which can lead to auditory or vestibular damage. Hearing impairment is projected to affect over 2.5 billion people worldwide by the year 2050[1]. While traditional treatments such as hearing aids and cochlear implants help mitigate these impairments, the recent demonstration of gene therapies has opened new avenues for treating genetic hearing loss[2–4]. In late 2023, the first pediatric patients received a viral-mediated therapy to partially restore genetic hearing loss, highlighting the need for reliable human models to evaluate new therapeutics[5]. Similarly, the national and global burden of vestibular dysfunction is severe—in the USA alone, ~35% of individuals over the age of 40 years experience some level of balance dysfunction[6].

Pathologies that lead to hearing loss often also result in vestibular dysfunction owing to similar cell types and functional overlap, as seen in genetic conditions such as Usher syndrome, Menière's disease and several autosomal dominant forms of genetic hearing loss such as DFNA9[7]. To study these disorders, both animal models and stem cell-based systems are critical, as they recapitulate different aspects of inner ear pathology with varying degrees of fidelity[8]. Among these, human stem-cell-based approaches have emerged as a promising tool to generate inner ear tissue in vitro, enabling the study of human-specific disease mechanisms and regenerative potential. For example, the use of human pluripotent stem cell (hPS cell)-derived inner ear organoids (IEOs) provides a powerful platform to investigate inner ear regeneration and repair processes[9]. These organoids make it possible to model human cellular responses to genetic mutations or environmental insults, such as exposure to ototoxic drugs, without relying on scarce patient or donor tissue. Hair cell regeneration in humans has only recently been explored[8,10], and IEOs offer an opportunity to identify human-specific gene regulatory elements that may govern or prolong regenerative capacity in hair cells and neurons.

Here, we present our IEO protocol, which provides a stepwise approach to reliably generate human sensory epithelium containing vestibular hair cells from hPS cells (Figs. 1 and 2). To aid the reproduction of this approach, we provide detailed guidance and quality control checkpoint data for comparison (Figs. 3 and 4 and Table 1). We present this protocol as an extension to our previous skin organoid protocol, Lee et al. 2022, to highlight the notable similarities and differences between these protocols[11,12]. Our aim is to facilitate the adoption of the IEO methodology by others in the field, which may in turn accelerate the development of therapeutic interventions for individuals affected by hearing and balance disorders. Researchers in many basic and translational fields can utilize our method to generate IEOs for their studies. This protocol can be performed in any laboratory equipped with tissue culture hoods and incubators suitable for aseptic cell culture work by individuals trained in PS cell culture and cell differentiation techniques.

Development of the protocol

Human embryonic stem cells (hES cells) and human induced PS cells (hiPS cells) hold immense promise in otology for modeling development and disease, testing new drug therapies and providing a potentially limitless source of cells for cell-based therapeutic approaches[9,13–15]. While many differentiation techniques have been developed to derive a variety of cell and tissue types, particularly those of the gut and brain[16–18], these approaches often rely on two-dimensional monolayer cultures that lack the complex cell–cell and cell–matrix interactions present in vivo. By contrast, three-dimensional (3D) culture techniques enable cells to self-organize and better mimic natural developmental processes (Fig. 1a).

In recent years, the importance of 'codevelopment', where progenitor cells of multiple cell lineages develop together in culture, has emerged in the stem cell biology field as a critical requirement for proper formation of organoids that mimic their native organs. In particular,

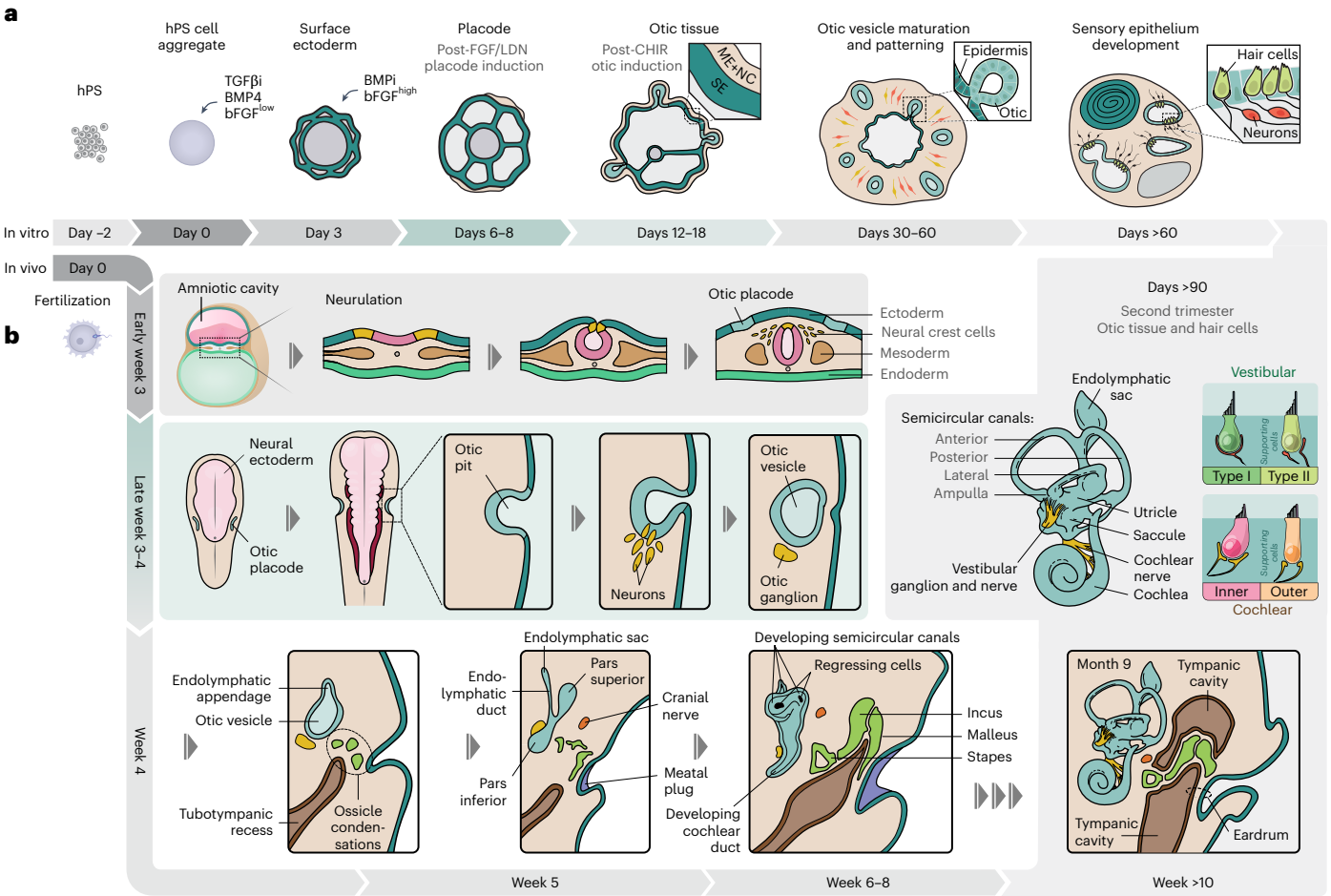

Fig. 1 | The IEO model recapitulates embryonic inner ear development. **a**, A timeline of in vitro otic tissue and sensory epithelium development in the IEO model. hPS cells form aggregates between day −2 and day 0. These aggregates are treated with TGFβ inhibitor (SB), BMP4 and a low concentration of bFGF on day 0, giving rise to the surface ectoderm by day 3. The aggregates are then treated with a BMP inhibitor (LDN) and a high concentration of bFGF, inducing the formation of the placode by days 6–8. A further treatment with CHIR starting at day 8 induces the otic tissue by days 12–18. The otic vesicle maturation and patterning occur during days 30–60, leading to the development of sensory epithelium, including hair cells and neurons, by day >60. Major off-target tissues, such as cartilage derived from cranial neural crest (NC) cells and epidermis originating from surface ectoderm (SE; nonneural ectoderm), commonly arise from NC cells within the mesenchymal (ME) layer and SE, which develop during days 12–18. **b**, A timeline of inner ear development in the human embryo. Neurulation occurs around 3 weeks of development, leading to the formation of the otic placode from the surface ectoderm. The otic pit forms from this placode, giving rise to the otic vesicle and early neurons by weeks 3–4. From week 4, the endolymphatic appendage and division of the otic vesicle occur, giving rise to the developing cochlear duct by week 5. Semicircular canals of the vestibular system develop through weeks 6–8, and these and other structures continue to mature up to 9 months of development.

the development of the inner ear seems to require complex epithelial–mesenchymal interactions[19–22]. Arising from a thickened patch of surface ectoderm (also known as nonneural ectoderm), the otic placodes invaginate into the head mesenchyme to form otic pits and then vesicles (also known as otocysts)[23–25] (Fig. 1b). This process of generating otic pits and vesicles has not been recapitulated using monolayer culture techniques[14,26,27]. Our IEO culture protocol, highlighted here and in our recent publications, successfully generates numerous otic vesicles on the surface of a floating 3D cell aggregate, each with the potential to form inner ear sensory epithelia[15,28–31] (Fig. 1). Since its development, our vestibular IEO protocol has proven to be a reliable method for generating vestibular-like IEOs with hair cells. This method has been successfully tested on more than ten cell lines in our laboratory and those of our collaborators[14,15,28,29].

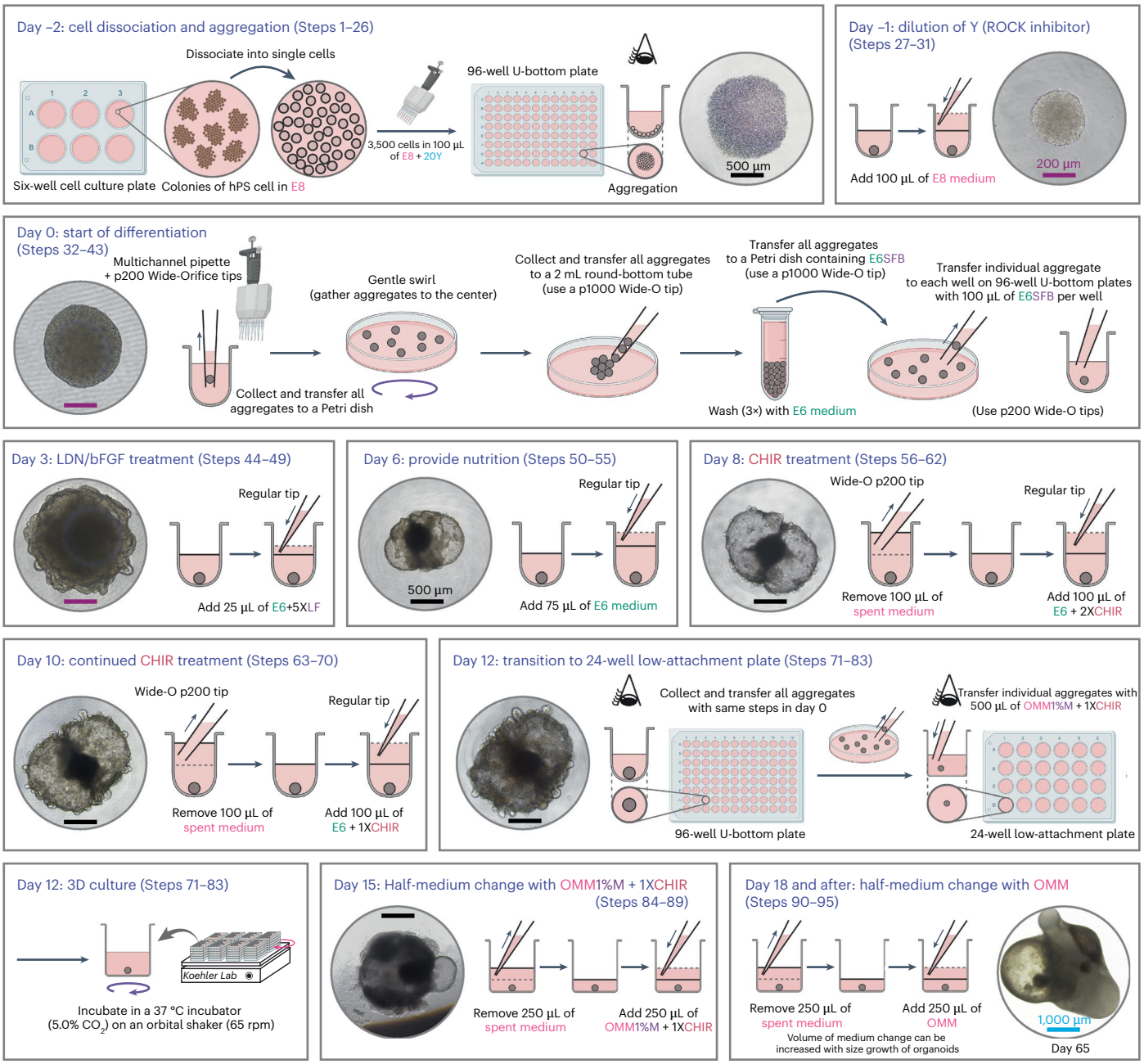

Fig. 2 | Illustration of stepwise treatments during directed differentiation of IEOs from day −2 through day 18 and beyond. Representative DIC images of SOX2-WTC hiPS cell-derived aggregates from day −2 to day 18 are shown. Day −2 (Steps 1–26): colonies of hPS cells in E8 medium are dissociated into single cells. In total, 3,500 cells are plated into each well of a 96-well U-bottom low-attachment plate in E8 containing a ROCK inhibitor (Y), leading to cell aggregation. Day −1 (Steps 27–31): Y is diluted by adding 100 µL of E8 medium to each well. Day 0 (Steps 32–43): the aggregates are collected in a 100 mm Petri dish and gently swirled to center them. The centered aggregates are transferred to a 2 mL round-bottom tube and washed three times with E6 medium. Aggregates are then transferred to a Petri dish containing E6 with SB, bFGF and BMP4 to start differentiation. Each aggregate is then transferred to an individual well of a 96-well U-bottom low-attachment plate. Day 3 (Steps 44–49): 25 µL of E6 containing LDN and bFGF is added to each well. Day 6 (Steps 50–55): 75 µL of E6 medium is added to each well to provide nutrients. Day 8 (Steps 56–62): 100 µL of spent medium is removed, followed by the addition of 100 µL of fresh E6 with CHIR. Day 10 (Steps 63–70): 100 µL of spent medium is removed and replaced with 100 µL of fresh E6 with CHIR to continue WNT activation. Day 12 (Steps 71–83): Aggregates are collected and transferred similarly to day 0. Individual aggregates are then transferred to each well of a 24-well low-attachment plate with 500 µL of OMM containing 1% Matrigel and CHIR. Plates are incubated in a 37 °C incubator (5.0% CO_2) on an orbital shaker (65 rpm). Day 15 (Steps 84–89): a half-medium change with OMM containing 1% Matrigel and CHIR. Day 18 and later (Steps 90–95): the spent medium is removed and replaced with fresh OMM. The volume of medium change can increase with the growth of the inner organoids. Scale bar, 200 µm (purple), 500 µm (black) and 1,000 µm (blue). This figure was prepared, in part, with resources available from Biorender.com.

Protocol extension

Our protocol is based on methodology first devised for generating neural and retinal organoids in the laboratory of Yoshiki Sasai, roughly between the years 2005 and 2013[32–39]. The groundbreaking studies by the Sasai group demonstrated that mouse PS cells and hPS cells, when formed into a cell aggregate, can form an outer layer of well-organized and polarized neuroepithelium. When these aggregates were supplied with extracellular matrix cues from Matrigel, they could spontaneously form retinal cup structures over the course of 2–3 weeks in culture. This original culture approach, known as the serum-free floating culture of embryoid body-like aggregates with quick reaggregation method served as the foundation for our culture platform[18].

To steer cells in serum-free floating culture of embryoid body-like aggregates with quick reaggregation cultures toward forming otic lineages, we tested a series of small molecules and protein treatments to mimic the key signals shown to be critical for surface ectoderm, preplacodal ectoderm and otic placode induction[30,40,41]. Following a period of guided differentiation, the cell aggregates contain a mixture of epithelial, mesenchymal and neuroglial cells. These aggregates are then allowed to self-organize for a period of weeks to months in a medium we specially formulated, referred to as organoid maturation medium (OMM), to support a multitude of cell types[11,28–30]. This extended period of self-organization results in complex cell–cell interactions, including apical–basal polarization of sensory epithelial hair cells containing stereocilia, synapse formation between hair cells and neurons and the expansion of periotic mesenchymal cells surrounding the sensory epithelia, all of which are higher-order features of inner ear morphogenesis (Figs. 2 and 4–6).

The protocol presented here has been modified from the original version published by Koehler et al. in the year 2017[30], which also formed the basis for our skin organoid protocol (see below)[11]. Key modifications have been made to ease the adoption of the method to other research groups[28,29] (Fig. 2). Notably, we replaced the custom-made 'chemically defined medium' used during the first 12 d of differentiation with a widely used off-the-shelf medium: Essential 6 Medium (E6 Medium; available from Thermo Fisher Scientific or STEMCELL Technologies). E6 Medium is a chemically-defined medium that has been used in several recent stem cell differentiation protocols, primarily for neural organoid induction[42,43]. On the basis of our qualitative observations, the E6 Medium appears to effectively facilitate the transition of cells from pluripotency media. Specifically, it supports the transition from Essential 8 (E8) Medium (available from Thermo Fisher Scientific or STEMCELL Technologies) or mTeSR Plus (mTeSR$^+$) Medium (available from STEMCELL Technologies), which we use for maintaining PS cell cultures and initiating cell aggregation for differentiation. The E6 Medium offers several benefits, including decreased cell death following aggregation and increased differentiation success, probably resulting from reduced contamination risks and pipetting errors during medium preparation. This change has yielded greater consistency in differentiation culture outcome across both biological and technical replicates[28]. Furthermore, we have eliminated the need for V-bottom 96-well plates, which have been difficult to source since our 2017 publication. The current protocol uses U-bottom 96-well low-attachment plates, which are available from multiple vendors; however, we strongly recommend using the Thermo Fisher Nunclon Sphera or S-Bio brand plates ('Materials' section). On the basis of unpublished observations, other seemingly comparable 96-well U-bottom low-attachment plates generate highly variable organoids, possibly owing to variations in coating materials. In addition, we eliminated a cumbersome step that involved embedding cell aggregates individually in Matrigel droplets on day 12 of differentiation. Now, the experimenters can simply transfer individual free-floating cell aggregates into a 24-well low-attachment plate containing medium with 1% Matrigel, yielding comparable results for otic induction.

Overall and in summary, since our original publications demonstrating how this series of signaling modulations can induce mouse IEOs, in the year 2013[41], and human IEOs, in the year 2017[30], the methodology has been tweaked and refined in our lab and by others in the field[44–50]. While precise timing and media compositions may vary, the main procedure involves specific patterning molecules to induce the stepwise differentiation of otic tissue from PS cells (Figs. 1 and 2). This stepwise protocol includes: (1) the generation of surface ectoderm using

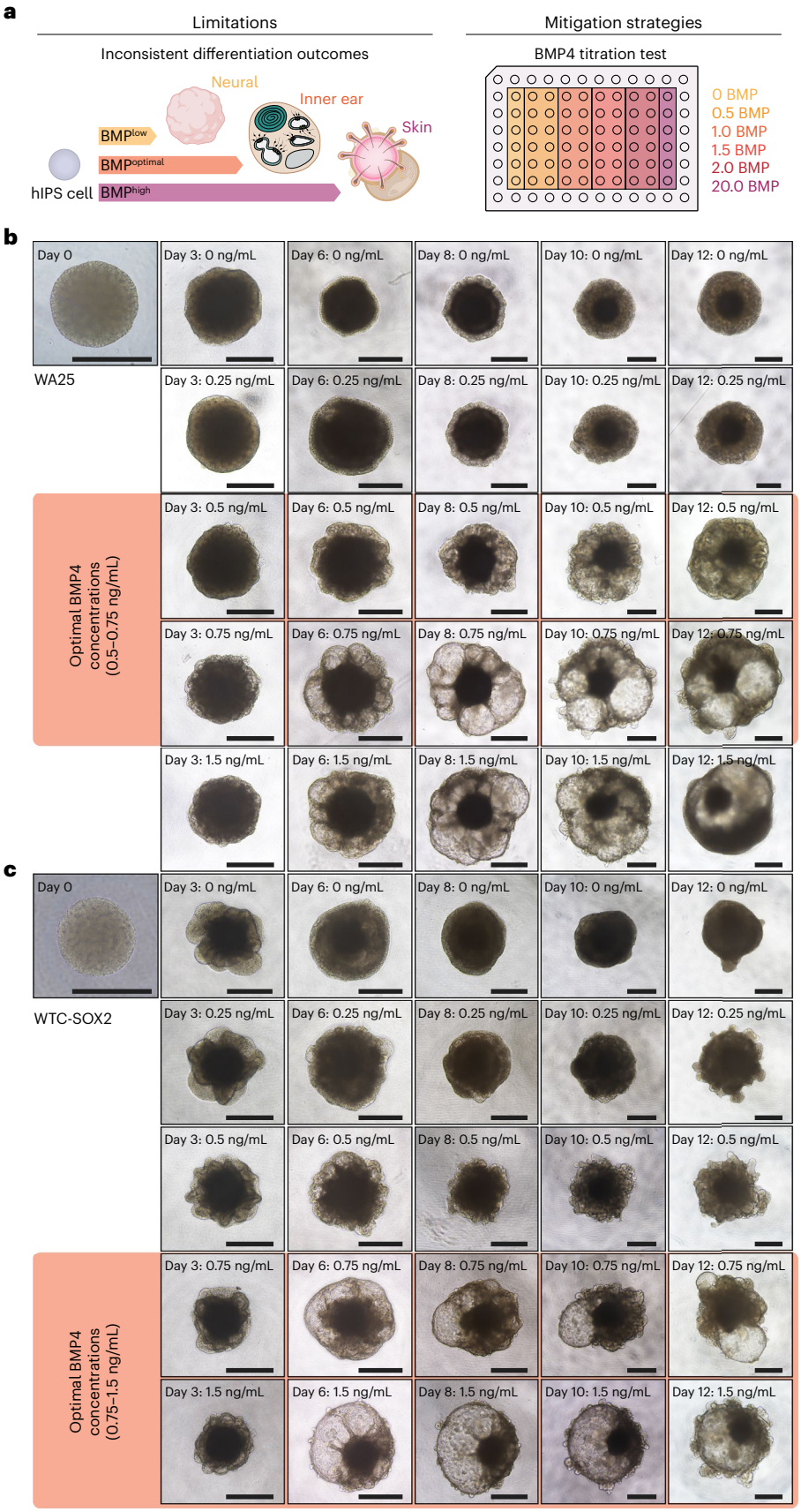
a
Limitations
Inconsistent differentiation outcomes
Neural
Inner ear
Skin
BMPlow
BMPoptimal
BMPhigh
hIPS cell
Mitigation strategies
BMP4 titration test
0 BMP
0.5 BMP
1.0 BMP
1.5 BMP
2.0 BMP
20.0 BMP
b
WA25
Optimal BMP4 concentrations (0.5–0.75 ng/mL)
c
WTC-SOX2
Optimal BMP4 concentrations (0.75–1.5 ng/mL)
Day 0
Day 3: 0 ng/mL
Day 6: 0 ng/mL
Day 8: 0 ng/mL
Day 10: 0 ng/mL
Day 12: 0 ng/mL
Day 3: 0.25 ng/mL
Day 6: 0.25 ng/mL
Day 8: 0.25 ng/mL
Day 10: 0.25 ng/mL
Day 12: 0.25 ng/mL
Day 3: 0.5 ng/mL
Day 6: 0.5 ng/mL
Day 8: 0.5 ng/mL
Day 10: 0.5 ng/mL
Day 12: 0.5 ng/mL
Day 3: 0.75 ng/mL
Day 6: 0.75 ng/mL
Day 8: 0.75 ng/mL
Day 10: 0.75 ng/mL
Day 12: 0.75 ng/mL
Day 3: 1.5 ng/mL
Day 6: 1.5 ng/mL
Day 8: 1.5 ng/mL
Day 10: 1.5 ng/mL
Day 12: 1.5 ng/mL

Fig. 3 | BMP4 titration for optimizing differentiation success. a, Limitations and mitigation strategies of BMP4 concentration optimization in IEO differentiation. Left: the range of differentiation outcomes from hPS cells based on different BMP4 activity levels, highlighting potential tissue types, including neural, otic and epidermal tissues, formed as a result of both applied and endogenous BMP4 expression. Right: a schematic of the BMP4 concentration test setup in a 96-well plate, used to optimize differentiation conditions for achieving desired outcomes. **b**, Morphology of the WA25 hES cell-derived aggregates at different BMP4 (Peprotech) concentrations: representative brightfield images show the progression of differentiation from day 0 to day 12. The aggregates were treated on day 0 with BMP4 at different concentrations of 0, 0.25, 0.5, 0.75 and 1.5 ng/mL. The images display morphological differences at days 3, 6, 8, 10 and 12. The light-orange background highlights the optimal BMP4 concentrations for WA25. **c**, A morphology of WTC-SOX2 hiPS cell-derived aggregates at different BMP4 concentrations; a similar setup to WA25, showing the differentiation from day 0 to day 12. Aggregates were treated on day 0 with the same BMP4 at different concentrations of 0, 0.25, 0.5, 0.75 and 1.5 ng/mL. Representative images illustrate morphological changes at days 3, 6, 8, 10 and 12. The light-orange background highlights the optimal BMP4 concentrations for WTC-SOX2. Scale bars, 500 µm.

low concentrations of basic fibroblast growth factor (bFGF) and bone morphogenetic protein 4 (BMP4) along with the inhibition of transforming growth factor-β (TGFβ) signaling, (2) the induction of otic placode tissue through a high concentration of bFGF treatment and inhibition of BMP signaling and, finally, (3) the specification of otic-epibranchial placode domain (OEPD)-like cells and otic placodes through persistent activation of WNT signaling. The final WNT signaling activation step is consistently shared across all IEO protocols.

Notably, the induction of surface ectoderm (stage 1 above) is a critical initial step on the path toward successful IEO generation and a prerequisite for success in subsequent steps. This step also appears to be a common challenge for labs new to the methodology. In many cases, the degree of success depends on delivering the precise amount of BMP4, as both the concentration and duration of BMP4 exposure are critical for generating surface ectoderm progenitor cells capable of subsequently forming posterior placodal and otic progenitor cells (Figs. 3 and 4 and Extended Data Fig. 1). Insufficient BMP4 concentrations will yield neural ectoderm with neuroepithelial tissue similar to that generated by neural organoid protocols, as observed in our no (0 ng/mL)-BMP4 controls[51,52] (Figs. 3 and 4 and Extended Data Fig. 1). Conversely, excessively high BMP4 concentrations, especially without the WNT pathway agonist CHIR99021 (CHIR), will result in the exclusive development of hair-bearing skin organoids (SKOs) such as those produced following our Lee et al. 2022 protocol[11,12]. For any new cell line, we recommend that experimenters perform a BMP4 concentration test (described in the 'Experimental design' section) to assess the optimal BMP4 concentration for successful IEO differentiation.

Comparison with other methods

Alternative approaches, such as animal models and primary tissue-derived human inner ear cultures are available; however, each approach faces significant limitations. Although significant progress has been made in modeling human genetic deafness in mice, these models often fail to fully capture the human phenotype[53]. While these models have been invaluable for inner-ear biology research, they have significant limitations owing to biological differences from humans in development, maturation and anatomy. Concerning the vestibular organ, while many vertebrates share a similar structure in their vestibular organs, consisting of two otolith-bearing end organs called the utricle and saccule and three semicircular canal cristae, their orientation, relative position and size vary across species. Moreover, the vestibular organs are of high interest in studying hair cell regeneration[8]. Although the vestibular end organs exhibit greater regenerative potential than the cochlea, the degree of hair regeneration appears to vary widely across species.

There are also differences between auditory systems across vertebrates. For example, mice begin hearing postnatally, while humans are born with functional hearing. In addition, mice have a higher auditory range, detecting up to 100 kHz compared with the 20 kHz upper limit in humans[53]. While many gene variants linked to nonsyndromic hearing loss in humans can alter hearing in mice, gene variants linked to complex syndromic forms often do not accurately reflect the corresponding human conditions[54]. Moreover, the development of therapies based on mouse disease models contributes to the high failure rate in the 'valley of death' phase of pharmaceutical development when transitioning to human testing.

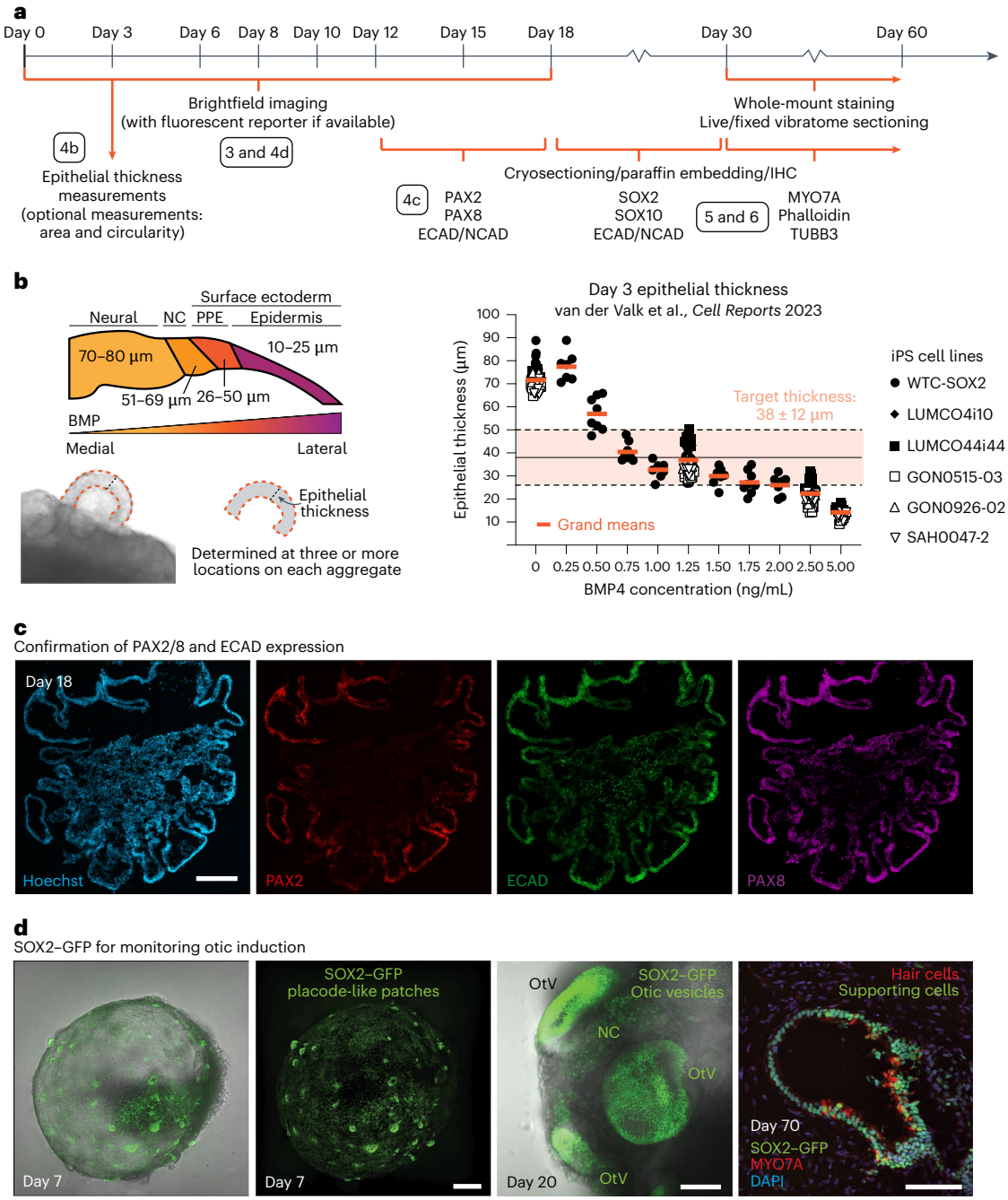

Fig. 4 | Key evaluation checkpoints and indicators of differentiation success. **a**, Schematic of the experimental timeline for organoid development and analysis. Key timepoints across IEO differentiation days 0–60 and beyond for brightfield imaging, epithelial thickness measurements, cryosectioning and paraffin embedding, as well as whole-mount staining and live/fixed vibratome sectioning, are indicated. Specific markers for IHC at various time points include PAX2, PAX8, SOX2, SOX10, ECAD/NCAD, MYO7A, Phalloidin and TUBB3. The circled figure callouts indicate the location of example data. **b**, A replotting of quantitative analysis from van der Valk et al. 2023 showing the epithelial thickness at day 3 across different BMP4 concentrations for various iPS cell lines[28]. Concentrations tested on all cell lines: 0, 1.25, 2.50 and 5.00 ng/mL. Concentrations tested on WTC-SOX2 line: 0, 0.25, 0.50, 0.75, 1.00, 1.25, 1.50, 1.75, 2.00, 2.50 and 5.00 ng/mL. Note that the target epithelial thickness range, 38 ± 12 µm was determined by the absolute range of values observed across cell lines at the 1.25 ng/mL level. The data are presented with the grand mean across all cell lines (n = 8–10 organoids per condition, each point the average of 3–4 epithelial measurements). **c**, Immunohistochemistry (IHC) staining of a day 18 WA25 organoid, treated with 0.5 ng/mL BMP4 on day 0. Representative images display ECAD$^+$ otic epithelia with PAX2$^+$ early stage and PAX8$^+$ intermediate-stage otic progenitors. **d**, Representative data from Steinhart et al. 2023 (ref. 29), highlighting the SOX2–GFP signal in otic lineage cells at various stages of IEO differentiation. Scale bars, 100 µm for **d**, 150 µm for **c**. **d** was reproduced from ref. 29, under a Creative Commons license (CC BY 4.0).

Table 1 | Key checkpoints in IEO differentiation

Stages	Media	Critical factors	Evaluation methods	Considerations or anticipated results	How often?
Day −2	E8 Flex or mTeSR$^+$	Y-27632	Brightfield microscopy	Optimal starting condition: 75–80% confluent, undifferentiated and healthy PS cells; critical for consistent and high-quality differentiation outcome	Every differentiation
Day 0	E6	bFGF BMP4 SB-431542 2% Matrigel	Brightfield microscopy	Formation of consistently sized spherical aggregates	Every differentiation
			BMP4 titration	Optimal factor concentration (particularly, BMP4) varies between cell lines, vendors and their lots	When introducing a new cell line or using BMP4 from a different lot
Day 3	E6	bFGF LDN	Brightfield microscopy	Development of surface ectoderm (bright/translucent) and inner core of neural ectoderm (dark)	Every differentiation
			Immunohistochemistry	ECAD$^+$ TFAP2A$^+$ outer surface ectoderm NCAD$^+$ PAX6$^+$ inner neural ectoderm	Optional
Days 6–10	E6	3 µM CHIR (day 8, day 10)	Brightfield microscopy	Aggregate size increases with a developing outer epithelium (bright/translucent thin layer) with placodes and dense inner core (dark)	Every differentiation
			Immunohistochemistry	PAX8$^+$ posterior placode versus OTX2$^+$ anterior placode in the outer epithelium	Optional
Day 12	OMM	3 µM CHIR 1% Matrigel	Brightfield microscopy	Otic pits and vesicles bulging outwards	Every differentiation
			Immunohistochemistry	PAX2$^+$ PAX8$^+$ otic pits and vesicles	When introducing a new cell line or assessing BMP4 titration
Days 15–18	OMM	3 uM CHIR (day 15) 1% Matrigel (day 15)	Brightfield microscopy	Outward expansion of mesenchymal cells engulfing the developing otic pits and pinching-off vesicles	Every differentiation
Day 21	OMM		Brightfield microscopy	Presence of donut-shaped otic vesicles within the aggregate	Every differentiation
			Immunohistochemistry	ECAD$^+$ SOX10$^+$ otic vesicles	When introducing a new cell line or assessing BMP4 titration
Day 40 and later	OMM		Brightfield microscopy	Maturation of otic vesicles into inner ear vesicles which increase in size with varying thickness of epithelium Off-target tissue development, including skin and cartilage, may be observed	Every differentiation
			Immunohistochemistry	Inner ear vesicles contain MYO7A$^+$ hair cells connected to TUBB3$^+$ neurons	When introducing a new cell line or assessing BMP4 titration

Therefore, there is a critical need for human models of inner ear development and the inner ear itself to effectively translate the findings from animal models into new therapies for human disease. However, access to the inner ear is restricted, and its regenerative capacity is minimal. Consequently, human inner ear cultures are typically confined to tissues that are either diseased or obtained postmortem, constraining the scope of experiments that can be conducted[55,56]. It is important to note that while IEOs made in the laboratory can recapitulate many of the features found in the native human inner ear, most notably, the cell diversity that makes up the sensory epithelium and its environment, IEOs do not yet model all the features found in the human system.

Finally, regarding the protocols for generating inner ear tissue from stem cells, timing and media composition have and may continue to evolve, as subtle differences in these factors can significantly impact differentiation outcomes (see the 'Experimental design' section for more details). Our colleagues in the laboratory of Eri Hashino at the Indiana University School of Medicine have recently reported two additional signaling events that can be appended as additional treatment steps toward the end of this protocol on days 14, 16, 18, 20 and 22. Specifically, they introduced sonic hedgehog activation using a small molecule agonist, purmorphamine, and WNT inhibition through an inhibitor of endogenous WNT secretion, IWP-2 (ref. 45). These alterations mimic in vivo signaling cues that ventralize the otocyst and induce cochlear duct formation[57–61]. This is because otic vesicles in vivo develop a dorsal region and a ventral region. The dorsal portion gives rise to the vestibular apparatus, while the ventral portion gives rise to the cochlea.

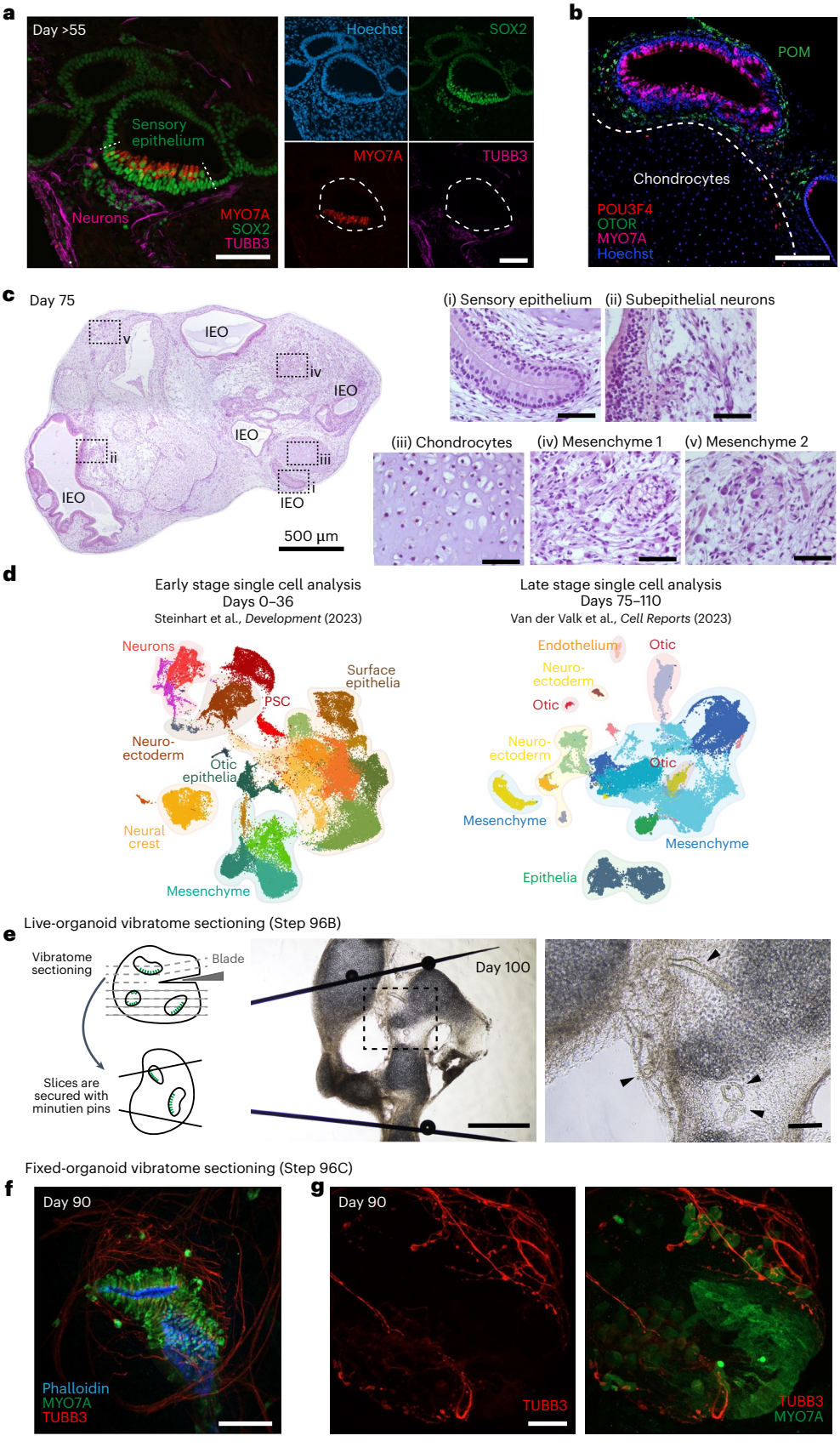
a
Day >55
Sensory epithelium
Neurons
MYO7A
SOX2
TUBB3
Hoechst
SOX2
MYO7A
TUBB3
b
POM
Chondrocytes
POU3F4
OTOR
MYO7A
Hoechst
c
Day 75
IEO
v
iv
IEO
IEO
ii
iii
i
IEO
IEO
500 µm
(i) Sensory epithelium
(ii) Subepithelial neurons
(iii) Chondrocytes
(iv) Mesenchyme 1
(v) Mesenchyme 2
d
Early stage single cell analysis
Days 0–36
Steinhart et al., Development (2023)
Late stage single cell analysis
Days 75–110
Van der Valk et al., Cell Reports (2023)
Neurons
Surface epithelia
PSC
Neuro-ectoderm
Otic epithelia
Neural crest
Mesenchyme
Endothelium
Otic
Neuro-ectoderm
Otic
Neuro-ectoderm
Otic
Mesenchyme
Mesenchyme
Epithelia
e
Live-organoid vibratome sectioning (Step 96B)
Vibratome sectioning
Blade
Slices are secured with minutien pins
Day 100
f
Fixed-organoid vibratome sectioning (Step 96C)
Day 90
Phalloidin
MYO7A
TUBB3
g
Day 90
TUBB3
TUBB3
MYO7A

Fig. 5 | Characterization of IEOs across differentiation stages. a, Representative IHC images of a day >55 organoid, showing MYO7A$^+$ hair cells, SOX2$^+$ supporting cells and TUBB3$^+$ neurons. The white dotted lines indicate the area of sensory epithelium, and the white dotted circle outlines the otic epithelium. **b**, High-magnification IHC images showing the MYO7A$^+$ hair cells along with POU3F4$^+$ and OTOR$^+$ periotic mesenchyme (POM) in organoids. These images highlight the structural organization and various cell types within the organoids for **a** and **b**. **c**, H&E staining images of a day 75 LUMC0044iCtrl44 organoid. The magnified insets i, ii, iii, iv and v show sensory epithelium, subepithelial neurons, chondrocytes and mesenchymal cells, respectively, providing a histological overview of diverse cell types and structures present at this stage. **d**, scRNA-seq and snRNA-seq uniform manifold approximation and projections (UMAPs). Day 0–36 scRNA-seq (left) adapted from Steinhart et al. (2023)[29] and day 75-110 snRNA-seq (right) adapted from van der Valk et al. (2023)[28]. These UMAPs illustrate the cellular diversity within organoids over time. **e**, A diagram of vibratome sectioning of organoids (left) and brightfield images of a D100 live vibratome-sectioned organoid slice (middle and inset of middle on right). These images depict the methodology for obtaining live-organoid sections that can be cultured for further analysis. The dotted box and rightmost image indicate the area containing inner ear tissue of interest, with arrowheads indicating the morphology of visible otic-like tissue. **f**, A representative IHC image of a fixed day 90 WA25 organoid that was sectioned at 150 µm thick, showing MYO7A$^+$ mature hair cells with Phalloidin$^+$ actin-rich hair cell bundles innervated by a complex network of TUBB3$^+$ neurons. **g**, High-magnification IHC images from the same conditions as **f** providing detailed views of neural structures within the organoids. Scale bars, 500 µm for **c**, left, 200 µm for **f**, 100 µm for **a**–**c** right insets i–v, 20 µm for **e** and **g**. **d**, left image, reproduced from ref. 29, under a Creative Commons license (CC BY 4.0). **d**, right image, reproduced from ref. 28, under a Creative Commons license (CC BY 4.0).

Using our protocol for IEO generation, we have observed mostly dorsal otic vesicle types and primarily vestibular organ-like development. This observation has been supported by using single-cell RNA-sequencing (scRNA-seq) analysis and validated at the protein level[28]. The Hashino group showed that ventralized IEOs yield cochlear duct-like sensory epithelia capable of forming hair cells with molecular features akin to outer cochlear hair cells[45]. While their pioneering work offers new insights into cochlear specification, the ventral IEO protocol was primarily developed using one hES cell line (WA25) with minimal validation in a healthy control hiPS cell line and will require further validation across additional PS cell lines. One major research goal in generating IEOs with various identities will be to increase the yield of otic epithelial cells in IEO cultures and precisely control the nonsensory and sensory patterning, as well as the cochlear versus vestibular patterning. Combining techniques to expand or purify otic progenitor populations with cochlear induction protocols could facilitate more extensive studies of genetic disorders impacting cochlear development.

Applications of IEOs

Modeling the early development of human inner ear and other cranial sensory cells

In vertebrate development, cranial placodes arise in a cranial region of the ectoderm at the border of the neural and surface ectoderm, an area known as the preplacodal area (Fig. 1b). Cranial placodes give rise to sensory neurons and epithelia[62]. Anterior placodes include adenohypophyseal (anterior pituitary), olfactory, lens and trigeminal placodes and posterior placodes include the otic and epibranchial placodes[63]. There are three epibranchial placodes in the human, and they give rise to neurons of the facial (VII), glossopharyngeal (IX) and vagal (X) cranial nerves (Fig. 1b). Cranial placode and otic vesicle development has been studied in zebrafish, chick and rodent models, providing a wealth of knowledge about the development of inner ear cell types[24,64]. The derivatives of the otic placode include all inner ear epithelia, such as sensory hair cells, supporting cells and neurons of the cranial vestibulocochlear nerve[65] (VIII; Fig. 1b). Recent publications have used scRNA-seq to show that our protocol, or protocol variants in other labs, yields cell aggregates containing a diversity of cranial cell types in the general region of the human fetal inner ear[28,29,31,66,67]. In our recent effort to create a single-cell developmental cell atlas of early-stage IEOs[29], we demonstrated that, in addition to otic placodes, our IEO cultures contain minor populations of anterior-like placodal epithelia and epibranchial-like placodes and neurons. This suggests that the IEO model may be a useful starting point for investigations into other placodes in addition to the otic lineage.

Although the inner ear is primarily derived from the otic vesicle, important signaling factors are supplied by other tissue types, such as the neural crest and the neural tube in vivo[24,68–71]. During our characterization of the IEO system, we have observed the derivation of these cell types within the multilineage aggregate[29]. In addition, the neural crest not only provides important signaling factors to the otic vesicle but also has a crucial role in providing myelination to the neurons of the cochleovestibular cranial nerve. We have ultrastructural evidence of the interaction between neural crest-derived Schwann cells and sensory neurons projecting to the

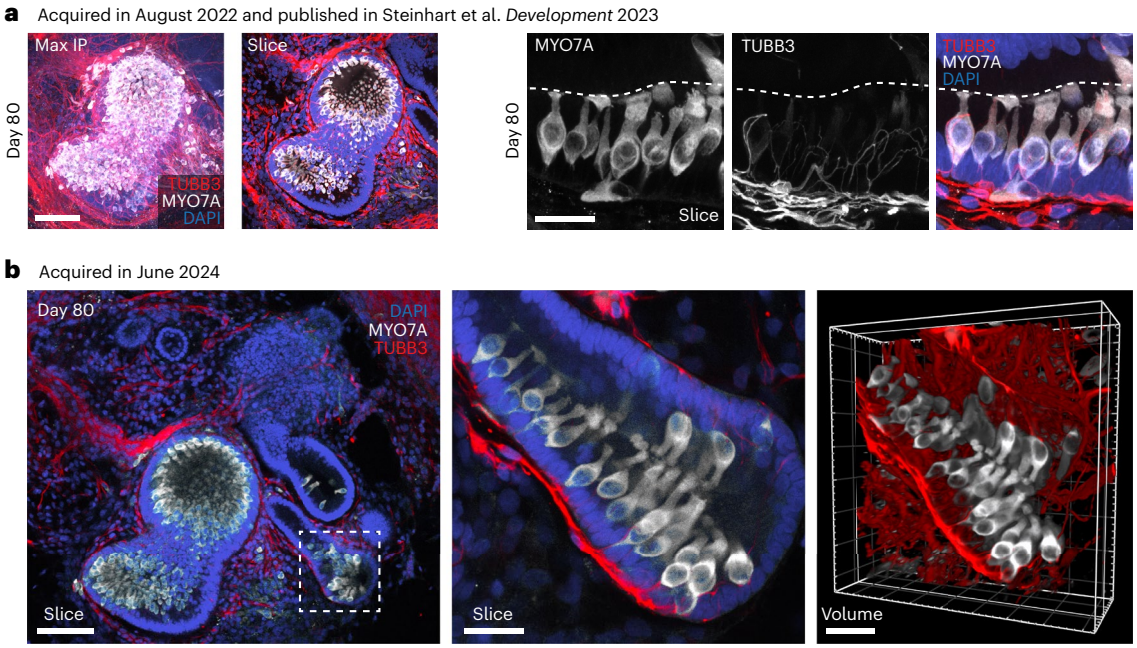

Fig. 6 | Long-term imaging of cleared organoids using the SHIELD protocol. **a**,**b**, Confocal images demonstrating the efficient long-term preservation of fluorescence signals in SHIELD-mounted organoids. The same sample was initially imaged in 2022 (**a**) and reimaged 2 years later in 2024 (**b**). All images were acquired using confocal microscopy with *z*-stack imaging and displayed as maximum intensity projections (max IP) or individual *z*-slices. The confocal images of a SHIELD-processed day 80 organoid stained for TUBB3$^+$ neurons (red) and MYO7A$^+$ hair cells (white) for **a**. Left: maximum intensity projection displaying the overall structure of the organoid. Second from the left: single *z*-slice (cross-sectional view) extracted from the *z*-stack, revealing the internal cellular organization. Right: high-magnification images of the cross-section showing MYO7A$^+$ hair cells, TUBB3$^+$ neurons and their merged signal, illustrating neuronal incorporation into hair cells. These images demonstrate the detailed architecture and cellular organization within the organoids. Confocal images of the same day 80 organoid reimaged 2 years later, demonstrating preserved fluorescence for **b**. Left: single *z*-slice from the *z*-stack, closely matching the cross-sectional view in **a**, second from the left. Middle: high-magnification view of the dotted box in the left, corresponding to the right in **a**. Right: volume-rendered *z*-stack of the middle, revealing the intact 3D structure of MYO7A$^+$ hair cells (white) and TUBB3$^+$ neurons (red). The persistence of fluorescence signals confirms the SHIELD protocol's effectiveness in stabilizing both the organoid structure and fluorophores for long-term imaging. Scale bars, 100 µm for **a** left two and **b** left, 25 µm for **a** right three and **b** right two. **a** was reproduced from ref. 29, under a Creative Commons license (CC BY 4.0).

developing otic vesicles in vitro, hinting at the potential for myelination[28]. Future studies may benefit from coculturing IEOs with brainstem-like cells or neural organoids to better support functional maturation and synaptic connections[72–74].

Disease modeling

A reliable protocol deriving cranial placode tissue, including otic vesicles, from hPS cells in vitro provides an excellent platform for researchers to model development as well as to analyze the mechanisms of genetic disease. Decades of research on human and murine genomes have identified more than 120 genes linked exclusively to nonsyndromic hearing loss and many others causing syndromic hearing loss, though the underlying mechanisms and human-specific nuances remain poorly understood[75]. For instance, various mouse models of Usher syndrome lack both the auditory and ocular phenotypes characteristic of the human pathology[76].

A notable example of disease modeling includes the study on CHARGE syndrome, in which human-specific and functional knockout mutations in the *CDH7* gene across various hiPS cell lines implicated this gene as critical for proper inner ear development[67]. Therapeutically, researchers were able to show that one only a fraction of cells need to express *CDH7* correctly to recapitulate proper development, encouraging the development of gene replacement strategies that do not necessarily require delivering the correct CDH7 coding sequence to the entire otic progenitor population.

A multilineage model might be ideal for identifying mechanisms involving hair cell-adjacent cell types, such as supporting cells, mesenchymal cells and neurons. This approach

could be particularly effective for modeling diseases that affect specific cell types, such as deafness caused by *GJB2* and *GJB6* mutations impacting supporting cells or *COCH* mutations primarily affecting mesenchymal cells[77–79]. For example, our cell–cell interaction analysis revealed potential crosstalk between hair cells and endothelial cells in the developing inner ear[28]. Many genetic deafness disorders arise during the development and maturation of the otic vesicle, such as branchiootorenal syndrome, which affects the embryonic development of the neck, ear and kidney. Generating in vitro otic vesicles within a multilineage aggregate that develops in an in vivo-like manner will enable close examination of key epithelial, mesenchymal and neuroglial cell types affected by genetic mutations.

Lastly, in vitro sources of specific cell types, such as those that develop in the cranial placode and otic vesicle, could potentially provide an unlimited source of cells for regenerative cell-based therapies. For gene-targeting therapies, the organoid model would offer an ideal platform to test viral capsid tropism and assess the cell type-specificity of promoters driving transgene expression[56].

Limitations

Despite the significant promise and advancements of IEOs, several limitations remain that researchers must consider. A primary limitation is the incomplete maturation and functionality of stem cell-derived organoids. While IEOs probably replicate many features of human inner ear vestibular organs[28], they do not fully capture the complex architecture of fluid-filled compartments, the spiral-shaped cochlea or the semicircular canals. Furthermore, functional assays, such as the patch-clamp electrophysiology used in our earlier studies on mouse IEOs, have been difficult to adapt for human IEOs owing to extended development times and the encapsulated structure of IEO cultures[30,41,80] (Fig. 5c). The vibratome sectioning approach presented here is one step toward addressing this issue by improving access to sensory epithelia for functional testing.

Although hair cells are polarized and form synaptic connections with a subepithelial compartment containing otic mesenchymal and endothelial cells[28], the intricate architecture of striolar versus extrastriolar or bulb-shaped ampullar sensory epithelium has not clearly been shown to be consistently replicated in the model, restricting the utility of IEOs in mechanistic studies of inner ear function. Future advancements may incorporate microfluidic systems (for example, PREDICT96 and Emulate chips)[81,82] or Transwell setups to allow better access to the apical surface of the sensory hair cells, enabling functional assays that are currently challenging owing to IEO tissue structure. In addition, the structural complexity of IEOs is simplified compared with the human inner ear, lacking critical apical structures, such as the otolithic membrane or tectorial membrane in the vestibular or cochlear organs, respectively. It is unclear whether the cell types essential for maintaining the ionic concentration of the endolymph are present in a sufficient degree to regulate and change the composition of the vesicle lumens to physiologically mature endolymph[28]. This simplification limits the ability of the model to represent the full spectrum of inner ear pathologies.

Another challenge is the variability in organoid formation and quality, both within and between batches, which affects the reproducibility and consistency in experimental results. On most occasions, we suspect that variability between repeated differentiations in the same cell line can arise from subtle activity differences across lots of BMP4, cell line passage numbers and experimenter skill levels. Distinctly and importantly, differences in BMP4 responsiveness across cell lines can vary; we suspect this is owing to differences in endogenous expression of BMP4. To optimize differentiation success, a BMP4 concentration test should be performed with new cell lines[28,31] (described in the 'Experimental design,' Figs. 3 and 4 and Extended Data Fig. 1).

Experimental design

For those interested in using this differentiation in their own laboratories, we address technical hurdles that laboratories may encounter when attempting this protocol for the first time. This includes a method for determining appropriate BMP4 concentrations (Fig. 3 and Extended Data Figs. 1 and 2) and standard antibody sets (Table 2) for quality control at various stages:

Table 2 | Primary antibodies

Primary antibody	Vendor	Cat. no.	RRID	Dilution	Host	Clonality	Ig isotype	Markers for:
ECAD	BD Biosciences	610182	https://scicrunch.org/resolver/RRID:AB_397581	1:50	Mouse	Mono	IgG2a	Epithelial tight junctions
MYO7A	Proteus	25-6790	https://scicrunch.org/resolver/RRID:AB_10015251	1:500	Rabbit	Mono	IgG1	Hair cells
OTOR	Invitrogen	PA5-55053	https://scicrunch.org/resolver/RRID:AB_2645111	1:100	Rabbit	Poly	IgG	Periotic mesenchyme
PAX2	Invitrogen	716000	https://scicrunch.org/resolver/RRID:AB_2533990	1:5	Rabbit	Poly	IgG	Early otic progenitors
PAX8	Invitrogen	MA1-117	https://scicrunch.org/resolver/RRID:AB_2536828	1:100	Mouse	Mono	IgG1	Intermediate otic progenitors
Phalloidin 488	Cytoskeleton	PHDG1A	n.a.	1:500	n.a.	n.a.	n.a.	F-actin/hair cell stereocilia bundles
Phalloidin 568	Biotum	00044-T	n.a.	1:500	n.a.	n.a.	n.a.	F-actin/hair cell stereocilia bundles
Phalloidin 647	Biotum	00041-T	n.a.	1:500	n.a.	n.a.	n.a.	F-actin/hair cell stereocilia bundles
POU3F4	This was a generous gift from Thomas Coate		n.a.	1:2000	Chicken		IgG	Hair cell progenitors
SOX2	BD Biosciences	561469	https://scicrunch.org/resolver/RRID:AB_10694256	1:100	Mouse	Mono	IgG1κ	Mature otic progenitors/ cerebral progenitors
SOX10	Invitrogen	PA5-47001	https://scicrunch.org/resolver/RRID:AB_2608449	1:20	Goat	Poly	IgG	Intermediate otic progenitors/ melanocytes
TUBB3	BioLegend	801202	https://scicrunch.org/resolver/RRID:AB_2313773	1:100	Mouse	Mono	IgG2a	β3 tubulin filaments

n.a., not available.

early differentiation (day 12), developing organoids (day 30) and mature organoids (>day 60) (Figs. 4–6 and Extended Data Fig. 1). For convenience, we will maintain an updated version of this protocol and other helpful resources at https://koehler-lab.org/resources.

Choosing a cell line

Human IEOs can be generated from hES cells or hiPS cells. Furthermore, these stem cell lines can be modified with fluorescent reporters, induced patient-specific mutations or conditional genetic perturbation strategies. Fluorescent reporter cell lines are a useful tool during the differentiation process as they can provide real-time feedback on cellular changes. Therefore, we recommend starting with one of these validated cell lines when initially establishing the organoid procedure in one's laboratory. Several cell lines are available from our laboratory upon request.

The choice of cell line is crucial for addressing specific experimental questions, as the tissue generated by this protocol is highly specific and sensitive to the timing and concentration of morphogens. Even subtle variations between cell lines can confound results. Here, we present a near-universal method (Figs. 1 and 2); however, the end users may need to implement small adjustments to the concentrations of the various small molecules and proteins to consistently generate IEOs. The specific yield of otic vesicle formation as well as the proportion of off-target tissues can vary depending on the cell line used[15,28]. Therefore, we advise conducting a pilot study to assess and optimize initial differentiation conditions, specifically, the BMP4 concentration needed to generate preplacodal ectoderm, before working with a new cell line. This is described more in detail in the following section. With WTC-based cell lines (discussed below), we typically observe that more than 90% of cell aggregates generate otic vesicles, with each aggregate producing ~5–10 otic vesicles visible under brightfield imaging and H&E staining in tissue sections (Fig. 5c).

In our experience, there are two key sources of variability that must be overcome to ensure high levels of rigor and reproducibility that arise during early stages of differentiation: (1) the varying levels of endogenous and exogenous levels of BMP4, attributed to differences in endogenous expression levels between cell lines and inconsistent activity of recombinant

BMP4 from different vendors; and (2) the consistency and accuracy in reconstituting recombinant proteins, such as BMP4 and bFGF. When attempting the protocol with a new cell line, we advise the end users to test a range of BMP4 concentrations (0–5 ng/mL for Peprotech BMP4) for the initial day 0 treatment, while keeping all other concentrations and treatment times constant (Fig. 3 and Extended Data Fig. 1). As shown, optimal BMP4 concentration is assessed by a combination of overall organoid morphology, early epithelial thickness and early immunohistochemistry profiling (Figs. 3 and 4; for more details, see the 'Key checkpoints for analysis' section). We observed that the optimal BMP4 concentrations can vary between hPS cell lines, influencing the differentiation coutcomes[28,30,31]. Specifically, some hPS cell lines require no BMP4 or varying concentrations to optimally differentiate into inner ear progenitors, contributing to the observed variability across lines[28,30]. We therefore recommend that the first-time users of this protocol acquire and use cell lines that have been previously validated by our group or other researchers. Moreover, we suggest routinely performing the BMP4 concentration test across different BMP4 batches to minimize the impact of lot-to-lot variability. When possible, the experimenter should plan for replication experiments to be initiated sequentially using BMP4 from the same lot. We find that optimal D0 BMP concentrations for most cell lines tend to be anywhere between 0.5 and 2.5 ng/mL. This value will be highlighted throughout the figures and text, as well as morphological and immunohistochemical metrics to determine optimal BMP concentrations.

Validated cell lines

We initially validated this protocol with the WA25 hES cell line from WiCell and observed that it requires a very low (or no) concentration of BMP4 to generate surface ectoderm and otic tissue[30] (Fig. 3b and Koehler et al. 2017). The parental WA25 cell line and the ATOH1–EGFP reporter line we previously derived from WA25 cells are excellent for generating IEOs[30]. Notably, the endogenous BMP4 activity of WA25 cells is unique, setting this cell line apart from any other lines we have tested[28,29] (Fig. 3 and van der Valk et al. 2023 and Steinhart et al. 2023).

As an alternative cell line, we have successfully adopted several fluorescently tagged hiPS cell lines developed by the Allen Institute for Cell Science (distributed by the Coriell Institute) in recent years and frequently use them for IEO generation. The parental WTC-11 (GM25256) cell line was derived from the skin fibroblasts of a healthy 30-year-old Japanese male, which were reprogrammed using episomal vectors (OCT3/4, shp53, SOX2, KLF4, LMYC and LIN28). The parental WTC-11 (GM25256) cell line can be purchased from the NIGMS Human Genetic Cell Repository at Coriell Institute for Medical Research (https://catalog.coriell.org/0/Sections/Search/Sample_Detail.aspx?Ref=GM25256&Product=CC). The donor of the WTC-11 line generously agreed to share whole-genome sequencing data with 100× coverage, which is ideal for designing gene-targeting strategies and evaluating single-nucleotide polymorphisms. These data are available on the Allen Institute website (https://www.allencell.org/genomics.html). One of the cell lines that we use in this protocol is WTC-mEGFP-SOX2-cl26 (SOX2–GFP), in which SOX2 is endogenously tagged with EGFP using a CRISPR–Cas9 editing approach. The SOX2–GFP labels PS cells, neuroectoderm, neural crest, otic placode and otic sensory epithelia in IEOs (Fig. 4d). In addition, we have previously shown that the desmoplakin–GFP (DSP–GFP) cell line is useful for monitoring IEO epithelia, as the GFP signal highlights the apical part of the otic and epidermal epithelia (Steinhart et al. 2023)[29]. Notably, each WTC-derived cell line has undergone a series of quality control checks by the Allen Institute, including the validation of precise gene editing by polymerase chain reaction and Sanger sequencing, tagged protein expression, stem cell marker expression (OCT4/SOX2/NANOG), karyotyping, exome sequencing and mycoplasma testing.

In addition to these WTC-based cell lines, we have successfully generated IEOs with the commercially available WA01 hES cell line (WiCell) and mND2-0 (WiCell) hiPS cell line, as well as multiple in-house generated cell lines, including the LUMC0004iCTRL10, LUMC0099iCTRL04, LUMC0044iCTRL44 (Leiden University Medical Center), GON0515-03, GON0926-02, SAH0047-02 (Boston Children's Hospital) and GMP-compliant hiPS cell lines[83]. We observed differences in the relative contribution of specific cell types between organoids derived from different iPSC lines[28], highlighting the inherent variability in cellular composition across lines. Although

we have successfully generated IEOs with dozens of cell lines, one cell line that has shown poor compatibility with this differentiation protocol is the WA09 (H9) hES cell line, which demonstrated very low efficiency and a preference for neural or neural crest induction under our culture conditions. We recently used the KOLF-2.1 line—a popular control line in the stem cell field[84]—to generate SKOs[85]. These results suggest that this line can generate nonneural ectoderm tissues and may serve as an excellent additional healthy control cell line for IEO generation.

Key checkpoints for analysis

The key checkpoints for differentiation are provided in Table 1. Throughout differentiation, morphological changes should be monitored under brightfield imaging (Figs. 2–4 and Extended Data Fig. 1). We have recorded the morphology at 40× and 100× magnification with an inverted Nikon Ts2R microscope equipped with a color camera, from single-cell seeding 2 d before directed differentiation (day −2) to day 18. The BMP4 concentration on day 0 needs to be optimized for different vendors and can be assessed by developing organoid morphology during the early days of differentiation as well as epithelial thickness measurements performed on images of the organoid taken on day 3 (Fig. 3 and Extended Data Fig. 1). The day 3 treatment is critical for expanding the preplacodal epithelium (PPE), and the thickness of the surface epithelium can be measured on this day as an early indicator of on-target sensory epithelium[28] (as highlighted in van der Valk et al. 2023 and Supplementary Figs. 1 and 4b). Optimal thicknesses can be measured through an imaging analysis program such as ImageJ or FIJI. Thicknesses between 26 and 50 µm (38 ± 12 µm) on day 3 appear to generate on-target progenitor tissue and are between the extremes of >75 µm (indicating neuroectoderm and cerebral fate) and <25 µm (preepidermis and skin fate). We provide one such example of a BMP titration experiment that produced varying epithelial thicknesses across multiple iPS cell lines (Fig. 4b).

Day 12 is also a key checkpoint to assess whether the aggregates are developing OEPD with restrained neural crest development. Distinct circular or 'donut-shaped' otic vesicles become visible at day 18 after CHIR treatment on days 8, 10, 12 and 15 (Figs. 2–4, Extended Data Figs. 1 and 2 and Table 1). Experimenters should use various key markers to assess organoid composition via immunostaining, including markers for the surface ectoderm (TFAP2A$^+$, ECAD$^+$ and NCAD$^-$), cranial placode (ECAD$^+$, NCAD$^+$ and SIX1$^+$), neural crest (NGFR$^+$ and SOX10$^+$) and neural tube (NCAD$^+$ and PAX6$^+$). The cranial placode portion of the cell aggregate gives rise to the otic vesicles that will mature to contain otic sensory epithelium (PAX2$^+$, PAX8$^+$, SOX2$^+$, ECAD$^+$ and SOX10$^+$) with hair cells (PCP4$^+$, MYO7A$^+$, POU4F3$^+$ and SOX10$^-$) and supporting cells (SOX2$^+$, MYO7A$^-$ and SPARCL1$^+$). Evaluating the E-cadherin (ECAD) and N-cadherin (NCAD) expression can be extremely useful in evaluating IEO cultures for successful induction of surface ectoderm (ECAD$^+$ and NCAD$^-$) or off-target neuroectoderm (ECAD$^-$ and NCAD$^+$). An ECAD$^+$ surface epithelium should be visible by day 3, with ECAD and NCAD coexpression appearing in the placodal and nascent otic epithelium by days 6–8 (see Table 2 for a list of markers that should be evaluated to validate new IEO cultures).

Downstream assays

Various late-stage downstream analysis methods can be employed to study IEOs, each providing unique insights into their development and functionality (Figs. 4a, 5 and 6). For fixed-tissue analysis, aggregates can be processed for cryo- or paraffin-embedding, followed by cryo- or thin-slice sectioning, histological and immune staining and imaging using widefield or confocal microscopy. This approach is suitable for imaging features of the organoid less than 25 µm in thickness (for example, cell morphology and cellular components). Alternatively, whole organoids can be stained using a modified SHIELD whole-mount staining protocol, described in detail in option A of Step 96 (refs. 86,87) (Fig. 6), which preserves the IEO architecture for confocal microscopy through stabilization, delipidation, antibody staining and refractive index matching. This approach is optimal for observing the overall features of the organoid as well as any regionalized or segregated tissues that may be present. In Fig. 6, we highlight the longevity of samples prepared using the SHIELD protocol by imaging a specimen that was prepared 2 years prior. As mentioned earlier, we have also implemented scRNA-seq

and single-nucleus RNA sequencing (snRNA-seq) approaches (Fig. 5d) to map the early fate decisions and developmental trajectories of inner ear tissue, as demonstrated in recent publications from our lab and in a collaborative study with Marta Roccio's group[31]. Publicly available developmental atlases based on our protocols enable comparative studies that show that the general landscape of cell diversity within organoids are similar across labs[45,66,67]. Lastly, both live and fixed organoids can also be sectioned with a vibratome, as described in options B and C of Step 96 (Fig. 5e). Live-tissue sections can be cultured for further functional applications such as patch-clamp electrophysiology, calcium imaging and FM dye uptake assays. Some limited electrophysiological measurements have been performed in microdissected tissue[30,45]; however, extensive functional testing across the timeline of hair cell and neuronal development in IEOs has not been performed and reported yet. Fixed sections are suitable for immunohistochemistry and imaging without clearing (Fig. 5f,g) and good for tissue features intermediate in size, around 60–240 µm in thickness (for example, neuron tracts). Together, these methods provide comprehensive tools for analyzing IEOs, facilitating a variety of experimental applications and potential protocol refinements.

Ethical considerations and institutional oversight

The use of hPS cells in biomedical research, including the generation of IEOs, involves important ethical considerations. The derivation and manipulation of hPS cells, whether from iPS cells or embryonic sources, must comply with local ethical guidelines for use of human cells[88]. These include obtaining informed consent from donors and following jurisdiction-specific policies governing the use of embryonic material. It is critical that all work involving hPS cells be conducted in accordance with national and international regulations, such as those outlined by the International Society for Stem Cell Research[88]. Institutional review board approval may also be required, depending on the specific requirements at the experimenter's institution. Most of the cell lines mentioned in this protocol are deidentified and approved for broad research use; however, experimenters should consult with their institution's legal team to execute the proper material transfer agreements and work with their local ethics review committee to receive the proper exemptions before initiating experimentation. This process can take several weeks to months.

Materials

Biological materials

PS cell lines

For the data presented in this protocol, hiPS cells and hES cells were obtained from commercially available and institutionally renowned sources, such as the Coriell Institute (https://www.coriell.org/1/Browse/Stem-Cells), the Allen Institute for Cell Science (https://www.allencell.org/cell-catalog.html) and the WiCell Research Institute (https://www.wicell.org/). hiPS cells were also generated by local core facilities, such as the F.M. Kirby Human Neuron Core at Boston Children's Hospital and Leiden hiPSC Centre at Leiden University Medical Center, using reprogrammed donor tissue. Cell lines that have been validated for generating IEOs include but are not limited to:

- The WA25 hES cell line (WiCell Research Institute) NIHhESC-12-0196, https://scicrunch.org/resolver/RRID:CVCL_E080, female
- The WA01 hES cell line (WiCell Research Institute) NIHhESC-10-0043 https://scicrunch.org/resolver/RRID:CVCL_9771, male
- The mND2-0 hiPS cell line (WiCell Research Institute) https://scicrunch.org/resolver/RRID:CVCL_U173
- The WTC-11 hiPS cell line (Allen Institute for Cell Science) and several fluorescently tagged hiPS cell lines developed from this parental line (notably, WTC11-mEGFP-SOX2-cl26)
- The LUMC0004iCTRL10 cell line (Leiden University Medical Center) https://scicrunch.org/resolver/RRID:CVCL_ZA10

- The LUMC0099iCTRL04 cell line (Leiden University Medical Center) https://scicrunch.org/resolver/RRID:CVCL_UK77
- The LUMC0044iCTRL44 cell line (Leiden University Medical Center)
- The GON0515-03, GON0926-02 and SAH0047-02 cell lines (Boston Children's Hospital)

▲ **CAUTION** The cell lines used in your research should be regularly checked to ensure that they are authentic and are not infected with mycoplasma. Detailed information on cell line validation and testing is available at https://www.wicell.org/home/stem-cells/catalog-of-stem-cell-lines/wa25.cmsx?closable=true and https://www.allencell.org/cell-catalog.html. We recommend repeated mycoplasma testing (Invivogen, cat no. rep-mys-10) throughout cell culture work, approximately every 3–4 months. Moreover, karyotyping of the iPS cell lines is recommended to ensure genomic stability of original cell stocks and after repeated passaging. Karyotyping is available through vendors such as Thermo Fisher (https://www.thermofisher.com/us/en/home/life-science/stem-cell-research/stem-cell-services/karyostat-karyotyping-service.html).

Reagents

Cell culture media and supplements

- E8 Flex medium (Gibco, cat. no. A2858501)
- E6 medium (Gibco, cat. no. A1516401)
- mTeSR$^+$ medium (STEMCELL Technologies, cat. no. 100-0276)
- Advanced Dulbecco's modified Eagle medium (DMEM)/F12 (Gibco, cat. no. 12634010)
- Neurobasal medium (Gibco, cat. no. 21103049)
- GlutaMAX supplement (Gibco, cat. no. 35050061)
- B-27 supplement, minus vitamin A (Gibco, cat. no. 12587010)
- N2 supplement (Gibco, cat. no. 17502048)
- 2-Mercaptoethanol (Gibco, cat. no. 21985023)

▲ **CAUTION** 2-Mercaptoethanol is considered toxic and can cause airway and skin irritation. Avoid contact with skin by using proper PPE and working with it inside of a biosafety cabinet.

- Normocin (InvivoGen, cat. no. ant-nr-1)

Cell dissociation and counting reagents

- 0.5 M ethylenediaminetetraacetic acid (Invitrogen, cat. no. 15575020)
- Accutase (Gibco, cat. no. A1110501)
- Trypan blue solution (Gibco, cat. no. 15-250-061)

Small molecules, proteins and matrices

- Vitronectin (Gibco, cat. no. A14700)
- SB431542 in solution (SB; Stemgent, cat. no. 04-0010-05)

▲ **CRITICAL** Light sensitive. Store in the dark at −20 °C as recommended by the manufacturer.

- Recombinant human bFGF (PeproTech, cat. no. 100-18B)
- Recombinant human BMP4 (PeproTech, cat. no. 120-05 and R&D Systems, cat. no. 314-BP; STEMCELL Technologies, cat. no. 78211 can be another option—refer to SKO protocol, Lee et al. 2022)[11].

▲ **CRITICAL** The activity of BMP4 may vary depending on the vendor, lot and in-lab handling (Fig. 3 and Extended Data Fig. 1). To ensure optimal activity, follow the vendor's datasheet for recommended reconstitution instructions. BMP4 treatments should be titrated when using a new vendor, lot or reconstituted vial to account for differences in potency. For consistent results across experiments, use the same BMP4 lot whenever possible.

- LDN-193189 in solution (LDN; Stemgent, cat. no. 04-0074-02)

▲ **CRITICAL** Light sensitive. Store in the dark at −20 °C as recommended by the manufacturer.

- CHIR in solution (Stemgent cat. no. 04-0004-02)
- Y27632 in solution (Y; Stemgent, cat. no. 04-0012-02)
- Matrigel, growth factor reduced (Corning, cat. no. 356231)

Protocol extension

Sample fixation and cryoembedding reagents

- 16% paraformaldehyde solution (PFA; Electron Microscopy Sciences, cat. no. 15710)
  ▲ **CAUTION** PFA is a potential carcinogen and should always be used in a fume hood.
- Sucrose (MP Biomedicals, cat. no. ICN19401891)
- Tissue freezing medium kit (Triangle Biomedical Sciences, cat. no. 15-183-36)
- Tissue Plus OCT compound (Fisher Scientific, cat. no. 23-730-571)

Live and fixed vibratome sectioning reagents

- Low melting point agarose (LMPA; Thermo Scientific, cat. no. 16520050)
- Hanks' balanced salt solution with calcium and magnesium (Gibco, cat. no. 14025092)
- Superglue (WB Mason, cat. no. GOR7805003)
- Sylgard (Fisher Scientific, cat. no. NC0162601)

Immunostaining and whole-mount staining reagents

- Normal goat serum (Vector Laboratories, cat. no. s-1000-20)
- Normal horse serum (Vector Laboratories, cat. no. s-2000-20)
- Prolong Gold antifade mountant (Invitrogen, cat. no. P369304)
- DAPI (Invitrogen, cat. no. D3571)
  ▲ **CAUTION** DAPI is potentially mutagenic and/or carcinogenic and should be handled with care.
- Hoechst (Invitrogen, cat. no. H3570)
  ▲ **CAUTION** Hoechst is potentially mutagenic and/or carcinogenic and should be handled with care.
- SHIELD Kit (contains: SH–SH–ON, epoxy, SH-Buffer and SH–ON) (Life Canvas Technologies, cat. no. SH-500)
  ▲ **CAUTION** Some components of the SHIELD kit are toxic and should be used as specified by the supplier.
  ▲ **CRITICAL** One of the components, 12.5% SHIELD-Epoxy-OFF, can be stored at 4 °C for up to 2 weeks.
- Sodium dodecyl sulfate (SDS; Millipore Sigma, cat no. L3771)
- Sodium borate (Millipore Sigma, cat no. 933953)
  ▲ **CAUTION** Sodium borate is potentially mutagenic and/or carcinogenic and should be handled with care.
- Sodium sulfite (Millipore Sigma, cat no. 239321)
- 5 M NaOH (Millipore Sigma, cat no. S8263)
  ▲ **CAUTION** Sodium hydroxide is caustic and should be handled with care and stored securely.

Buffers and other reagents

- 1× phosphate-buffered saline (pH 7.4) (PBS; Gibco, cat. no. 10010049)
- 1× Dulbecco's PBS (DPBS; Gibco, cat. no. 14190250)
- 10% Triton X-100 (Sigma-Aldrich, cat. no. 93443)
- Dimethyl sulfoxide (DMSO; Fisher BioReagents, cat. no. BP231-100)
- 1 M Tris–HCl, pH 7.5 (Fisher BioReagents, cat. no. BP1757-100)
  ▲ **CRITICAL** For reconstituting human recombinant bFGF from PeproTech, check the data sheet that is provided with lyophilized powder and the certificate of analysis for proper reconstitution instructions.
- Citric acid (Fisher Chemical, cat. no. A104-500)
  ▲ **CRITICAL** For reconstituting human recombinant BMP4 from PeproTech, check the data sheet that is provided with lyophilized powder and the certificate of analysis for proper reconstitution instructions.
- Hydrochloric acid (HCl; Thermo Fisher Scientific, cat. no. A144S-500)
  ▲ **CRITICAL** For reconstituting human recombinant BMP4 from R&D Systems, check the data sheet that is provided with lyophilized powder and the certificate of analysis for proper reconstitution instructions.

- Human serum albumin (HSA; Sigma-Aldrich, cat. no. A9731)
  ▲ **CRITICAL** Used as carrier protein for recombinant protein reconstitution, HSA is critical for a proper recombinant protein stability and efficacy.

Antibodies for immunostaining

- Primary antibodies: all primary antibodies can be found in Table 2.
- Secondary antibodies: all secondary antibodies are from the Alexa Fluor family, conjugated to 488, 568 or 647 fluorophores. A complete list of secondary antibodies can be found in Supplementary Table 1.

Equipment

For cell culture

- STERILGARD 404 E[3] (biosafety cabinet; Baker, cat no. SG404)
- MCO-170AICUVL-PA CellIQ (incubator; PHC Corporation of North America, cat no. MCO-170AICUVL-PA)
- CO_2-resistant shaker (Thermo Scientific, cat. no. 88881101)
- Universal aluminum platform for CO_2-resistant shaker (Thermo Scientific, cat. no. 88-881-122)
- Six-well culture plates (Corning, cat. nos. 353046, 3516 or Thermo Scientific, cat. no. 140675)
- U-bottom low-attachment 96-well plates (Thermo Scientific, cat. no. 174925 or S-Bio, cat. no. MS-9096UZ)
  ▲ **CRITICAL** Different coating materials used from different vendors affect the efficiency and quality of differentiation.
- Low-attachment 24-well plates (Thermo Scientific, cat. no. 174930)
  ▲ **CRITICAL** Different coating materials used from different vendors affect the efficiency and quality of differentiation process.
- Invitrogen Countess III FL automated counter (Invitrogen, cat. no. AMQAF2000)
- Disposable cell counting chamber slides for Countess automated cell counter (Invitrogen, cat. no. C10228).
- 10 mL reagent reservoirs (VistaLab Technologies, cat. no. 21-381-093)
- 25 mL reagent reservoirs (VistaLab Technologies, cat. no. 21-381-27D)
- 5 mL round-bottom polystyrene test tubes with cell strainer snap caps (mesh size 35 µm) (Corning, cat. no. 352235)
- 250 µL wide-orifice (Wide-O) LiteTouch System (LTS) pipette tips, low retention, sterile (Rainin, cat. no. 30389250)
- 1,000 µL Wide-O LTS pipette tips, low retention, sterile (Rainin, cat. no. 30389221)
- 100 mm bacteriological Petri dishes with lid (Falcon, cat. no. 351029)
- 2 mL Corning externally threaded cryogenic vials (Corning, cat. no. 430659)
- Corning CoolCell FTS30 cell freezing vial containers (Corning, cat. no. 432008)
- Corning CoolCell LX cell freezing vial containers (Corning, cat. no. 432002)

For reagent preparation

- pH meter (Mettler Toledo, cat. nos. 01-915-102, 01-917-142)
- Stirrer with ceramic plate, Isotemp 30 °C to 540 °C (Fisher Scientific, cat. no. FB30786163)
- Parafilm (Bemis, cat. no. PM996)
- Hamilton fume hood (Fisher Hamilton L.L.C., cat. no. 70864)
- 0.22 µm filter (Millipore Sigma, cat. no. SLGPR33RS)
- BD Slip tip 1 mL sterile syringes (Fisher Scientific, cat. no. 14-823-434)
  ▲ **CRITICAL** For filtering HSA solutions during recombinant protein reconstitution.

For cryosectioning and immunostaining

- Cryostat (Leica, cat. no. 149491860us)
- Tissue-Tek biopsy cryomolds 10 mm × 10 mm × 5 mm (Sakura Finetek, cat. no. 4565)
- Tissue-Tek intermediate cryomolds 15 mm × 15 mm × 5 mm (Sakura Finetek, cat. no. 4566)
- Desiccator (Thermo Scientific, cat. no. 53110250)
- Superfrost Plus slides (Fisher Scientific, cat. no. 12-550-15)

- 24 mm × 50 mm #1 Thickness Cover Glass (Fisher Scientific, cat. no. 22-050-233)
- PAP pen (Electron Microscopy Sciences, cat. no. 71310)
- Coplin jar (IHC World LLC, cat. no. IW2501C)
- Humidified slide staining chamber (Fisher Scientific, cat. no. NC9062083)
- 3D platform rotator (Fisher Scientific, cat. no. 88-861-045)
- Eight-well silicone isolators 2.0 mm (Electron Microscopy Sciences, cat. no. 70339-44)
- Eight-well silicone isolators 2.5 mm (Electron Microscopy Sciences, cat. no. 70339-46)
- 12-well glass bottom plate with high performance #1.5 cover glass (Cellvis, cat no. P12-1.5H-N)
- 24-well glass bottom plate with high performance #1.5 cover glass (Cellvis, cat no. P24-1.5H-N)
- 96-well glass bottom plate with high performance #1.5 cover glass (Cellvis, cat no. P96-1.5H-N)
- 35 mm Petri dish with 14 mm diameter glass bottom microwell (MatTek, cat. no. P35G-1.5-14-C)

For vibratome sectioning

- Leica vibratome VT1000S and Leica vibratome VT1200 (Leica Microsystems, cat. no. 140 4723 5612 and 140 4814 2065)
  ▲ **CRITICAL** A separate vibratome for fixed and live tissue is recommended to avoid cross-contamination and accidental fixation of live tissue.
- Disposable base molds (Fisher Scientific, cat. no. 22-363-553)
- Disposable transfer pipette (Thermo Scientific, cat. no. S304673)
- Vibratome sapphire blade (Delaware Diamond Knives, cat. no. SAFN)
- Minutien pins (Fine Science Tools, cat. no. 26002-10)
- 18 mm round coverslips (Thomas Scientific, cat. no. 1217N81)
- 12-well culture plate (Thermo Fisher Scientific, cat. no. 150628)
- 12-well glass-bottom plate (Cellvis, cat. no. P12-1.5H-N)
- Perforated metal spoon, diameter 20 mm (World Precision Instruments, cat. no. 501997)

For imaging and image analysis

- Nikon Ts2R (Nikon Instruments, cat. no. MFA34200)
- Nikon Ti2 (Nikon Instruments, cat. no. MEA54000)
- Nikon A1R (Nikon Instruments, cat. no. A1R-HD25 4-line Package)
- NIS-Elements Imaging Software (Nikon Instruments, cat. no. MQS31100)
- ImageJ (https://imagej.net/)

Common equipment

- Moria perforated spoon, diameter 15 mm (Fine Science Tools, cat. no. 1037018)
- Moria perforated spoon, diameter 20 mm (Fine Science Tools, cat. no. 10370-17)
- Kimwipes (Kimtech Science, cat. no. 34256)
- 0.6 mL snap cap low-retention microcentrifuge tubes (Thermo Scientific, cat. no. 3446)
- 1.5 mL snap cap low retention graduated microcentrifuge tubes (Thermo Scientific, cat. no. 3448)
- 2 mL round-bottom microcentrifuge tubes with locking snap cap (Fisher Scientific, cat. no. 14-666-315)
- 15 mL conical tubes (Thermo Scientific, cat. no. 12-565-268)
- 50 mL conical tubes (Thermo Scientific, cat. no. 12-565-270)
- 5 mL serological pipettes (Fisherbrand, cat. no. 13-678-11D)
- 10 mL serological pipettes (Fisherbrand, cat. no. 13-678-11E)
- 25 mL serological pipettes (Fisherbrand, cat. no. 13-678-11)
- 50 mL serological pipettes (Fisherbrand, cat. no. 13-678-11F)
- Starter kit including four LTS Pipet-Lite XLS+ manual single channel pipettes (Rainin, cat. no. 30386597)
- 20 µL LTS pipette tips, low retention, sterile (Rainin, cat. no. 30389229)
- 250 µL LTS pipette tips, low retention, sterile (Rainin, cat. no. 30389246)
- 250 µL LTS pipette tips, wide orifice, low retention, sterile (Rainin, cat. no. 30389250)
- 1,000 µL LTS pipette tips, low retention, sterile (Rainin cat. no. 30389216)
- 1,000 µL LTS pipette tips, wide orifice, low retention, sterile (Rainin cat. no. 30389221)

Table 3 | Key cell culture reagents

Chemical name	Function	Re-constitution	Storage	Stock conc.	Working conc.	Expiration date
bFGF	FGF growth factor	5 mM Tris–HCl (pH 7.6) with 0.1% HSA[a]	−80 °C	200 µg/mL	4 ng/mL (day 0) 50 ng/mL (day 3)	6 months from the date of reconstitution
BMP4	TGFβ-family growth factor	5 mM Citric Acid with 0.1% HSA[a]	−80 °C	100 µg/mL	0.5–2.5 ng/mL (day 0): Figs. 3 and 4	6 months from the date of reconstitution
		Sterile water with 0.1% HSA[a]	−80 °C	100 µg/mL	2.5 ng/mL (day 0): data not shown	3 months from the date of reconstitution
		4 mM HCl with 0.1% HSA[a]	−80 °C	100 µg/mL	15 ng/mL (day 0): Extended Data Fig. 1	3 months from the date of reconstitution
SB	TGFβ (ALK4, 5, 7) inhibitor	Already in DMSO	−20 °C	10 mM	100 µM (day 0)	6 months from the date received
LDN	BMP4 (ALK2,3) inhibitor	Already in DMSO	−20 °C	10 mM	200 nM (day 3)	6 months from the date received
CHIR	GSK-3 inhibitor (Wnt agonist)	Already in DMSO	−20 °C	10 mM	3 µM (days 8, 10, 12 and 15)	6 months from the date received
Y	ROCK inhibitor	Already in DMSO	−20 °C	10 mM	10 and 20 µM (day −2)	6 months from the date received
Vitronectin	Plate coating solution	Ready to use	−80 °C	500 µg/mL	5 µg/mL (hPS cell maintenance)	2 years from the date on the vial
B-27, minus vitamin A	Culture supplement	Ready to use	−20 °C	50×	0.5× (>day 12)	Date on the bottle
N2	Culture supplement	Ready to use	−20 °C	100×	0.5× (>day 12)	Date on the bottle
GlutaMAX	Alternative to L-glutamine	Ready to use	RT	100×	1× (>day 12)	Date on the bottle
2-Mercaptoethanol	Reducing agent	Ready to use	4 °C	50 mM	0.1 mM (>day 12)	Date on the bottle
Matrigel, growth factor reduced	Cellular basement matrix	Ready to use	−20 °C	100%	2% (day 0) 1% (days 12 and 15): thaw overnight on ice	2 years from the date of manufacture
Normocin	Antibiotic	Ready to use	4 °C	50 mg/mL	100 µg/mL	Date on the vial

conc., concentration. [a]Refer to data sheet for expiration of original stock vial, storage instructions for aliquots and accurate reconstitution instructions.

Reagent setup

The details on the reconstitution of human recombinant bFGF, human recombinant BMP4, STEMCELL Technologies BMP4, SB and LDN in solution as well as preparations of E8 Flex medium, E6 medium and E8 containing Y-27632 have been previously described[44]. These reagents are common across these two protocols, and there are no differences. The key cell culture reagents are briefly summarized in Table 3, and basal culture media required for hiPS cells and organoids across various differentiation stages and during maturation are outlined in Table 4. Organoid differentiation media, however, is modified to generate IEOs: its composition is specified in Table 5. Differentiation media that are applied on specific days should be prepared the same day as the treatment (ideally immediately before) to prevent the denaturation and loss of activity of small molecules and recombinant proteins and are included in detail in the protocol.

Procedure

▲ **CRITICAL** Certain features of working with hPS cell culture (including both hES cell and hPS cells) are common to protocols for generating hair follicle-bearing SKOs and IEOs. Detailed procedures for thawing, maintaining, passaging and freezing PS cells are described in detail in our earlier protocol for SKOs[44].

▲ **CRITICAL** Every step is performed in a tissue culture biosafety cabinet using appropriate biosafety level-2 personal protective equipment.

▲ **CRITICAL** Always prewarm media at room temperature (RT, ~20 °C) for 15–20 min. Do not warm the media in a water bath or 37 °C.

Table 4 | Basal culture media

Medium name	Function	Vendor	Cat. no.	Storage	Stock volume
E8 Flex medium	Support the pluripotency of PS cells	Gibco	A2858501	In stocks: 4 °C (medium), −20 °C (supplement) After mix: 4 °C	500 mL basal medium 10 mL supplement
mTeSR^{+} medium	Support the pluripotency of PS cells	STEMCELL Technologies	100-0276	In stocks: 4 °C (medium), −20 °C (supplement) After mix: 4 °C	400 mL basal medium 100 mL supplement
E6	Support differentiation of PS cells	Gibco	A1516401	4 °C	500 mL
Advanced DMEM/F-12	Basal medium	Gibco	12634010	4 °C	500 mL
Neurobasal medium	Maintain long-term culture	Gibco	21103049	4 °C	500 mL

Differentiation day (−2): cell dissociation and aggregation

● **TIMING 50 min**

▲ **CRITICAL** This protocol is standardized to the preparation of culture in two 96-well plates. Use cells that are 75–80% confluent.

Media and enzyme preparation

1. Prepare 10 mL and 22 mL of E8 Flex medium containing supplements in two separate conical tubes. Add 10 µL of Y to the 10 mL medium, which brings final concentration to 10 µM Y (hereafter, E8+10Y), and 44 µL of Y to the 22 mL medium, which brings final concentration to 20 µM Y (hereafter, E8+20Y). Then, equilibrate prepared media to RT.
2. Prewarm Accutase at RT or at 37 °C.
   ▲ **CRITICAL STEP** The use of 37 °C-prewarmed Accutase expedites the dissociation process, necessitating a shorter incubation time compared with the use of RT-prewarmed Accutase.

Cell dissociation

3. Aspirate out the spent medium of the cells in one well of a six-well culture plate.
4. Carefully wash with ~2 mL of 1× DPBS twice and aspirate out the 1× DPBS from the last wash.
5. Add 500 µL of prewarmed Accutase and incubate for 3–4 min in 37 °C incubator with 5.0% CO_2. After 2–3 min of the initial incubation, gently rock and shake the plate to detach any loose cells that are still adhering on the surface of the plate. Check under a microscope to confirm the detachment. If cell colonies are still attached tightly, incubate for additional 20 s increments until the cells are fully detached and partially single-celled.
6. Hold the plate at an angle and use a p1000 Wide-O tip to gently pipette the solution in both clockwise and counterclockwise directions within the well, collecting all detached single cells and cell clusters at the bottom.

Table 5 | OMM

Component	Stock concentration	Final concentration	Volume (total 100 mL)
Advanced DMEM/F12	–	49% (vol/vol%)	49 mL
Neurobasal medium	–	49% (vol/vol%)	49 mL
N2 supplement	100×	0.5×	500 µL
B27 supplement, minus vitamin A	50×	0.5×	1 mL
GlutaMAX	100×	1×	1 mL
2-Mercaptoethanol	55 mM	0.1 mM	182 µL
Normocin	50 mg/mL	100 µg/mL	200 µL

Remaining medium can be stored in 4 °C and used within 2 weeks of preparation.

7. While holding the plate at an angle, add 1 mL of E8+10Y to the top of the well, allowing any remaining cells to flow to the bottom. Pipette the solution at the bottom of the well with moderate force to dissociate any remaining cell clusters into single cells.
8. Transfer the dissociated cell suspension from the bottom of the well to a 15 mL conical tube, keeping the plate angled.
9. Add another 1 mL of E8+10Y to the well and repeat the process in Steps 7–8, allowing any remaining cells to flow to the bottom. Gently pipette at the bottom of the well, then transfer this cell suspension to the 15 mL conical tube from Step 8. The total volume of cell suspension should be ~2.5 mL.
10. Using a p1000 regular tip, gently pipette up and down within the conical tube to further dissociate any remaining cell clusters.
11. Using a 5 mL serological pipette, add an additional 3 mL of E8+10Y to the conical tube containing the single-cell suspension from Step 10, bringing the total volume to ~5.5 mL.
12. Centrifuge at 230*g* for 5 min 30 sec at RT to pellet the cells.
13. Carefully aspirate the supernatant by tilting the tube to allow the medium to flow away from the pellet.
    ▲ **CRITICAL STEP** Be cautious to not disturb the cell pellet.
14. Using a p1000 Wide-O tip, resuspend the cells in 1 mL of E8+10Y by gently pipetting up-and-down.

Cell aggregation

15. To equilibrate the 35 µm mesh of a cell strainer, use a p1000 regular tip to pipette 1 mL of E8+10Y through the strainer mesh with steady force.
16. Transfer the resuspended cells in 1 mL of E8+10Y from Step 14 to the equilibrated cell strainer, in a dropwise manner.
17. To ensure the thorough collection of cells, rinse the conical tube that contained the resuspended cells with 1 mL of E8+10Y, and transfer the rinse onto the cell strainer dropwise. This brings the total volume in the cell strainer tube to ~3 mL.
18. Gently tap the strainer tube on the surface of the biosafety cabinet to allow any droplets beneath the strainer mesh to fall.
19. Carefully remove and discard the snap cap, which contains the mesh component of the cell strainer.
20. Determine the number of live cells collected in the tube from Step 18 as follows:
    - Prepare 50 µL of trypan blue in a 500 µL tube
    - Using a p1000 Wide-O tip, pipette up-and-down to thoroughly mix the cell suspension in the strainer tube from Step 18
    - Immediately, using a p200 regular tip, collect 50 µL of cell suspension from the center of the volume in the tube and transfer it to the 50 µL of prepared trypan blue, creating a 1:1 dilution
    - Gently pipette to mix the cell suspension evenly with the trypan blue
    - Add 11 µL of the cell-trypan blue mixture to each side of a disposable cell counting chamber slide for the Invitrogen Countess III automated counter or onto a hemocytometer
    - Record the live cell number count per 1 mL shown on the automated counter. Note: The Invitrogen Countess III automated counter automatically calculates cell numbers considering the trypan blue dilution. For manual counting, multiply by two to account for the dilution factor
    - Calculate the number of cells needed for a differentiation experiment. A final concentration of 35,000 cells per mL (3,500 cells in 100 µL per well) is needed for a differentiation culture. To seed two full 96-well plates, prepare 22 mL of medium containing 7.7×10^5 cells
    - Then, calculate the volume of single-cell suspension needed for the experiment. For example, if the live cell count from the automated cell counter is 5×10^5 cells per mL, 1.54 mL of the cell suspension is needed in 22 mL of medium

- Equation $C_1V_1 = C_2V_2$
  - (Live cell count from counter in cells per mL) × (volume of single-cell suspension needed for differentiation in mL) = (desired cell concentration for differentiation, 0.35 x 10^5 cells per mL) × (total volume of medium needed for the differentiation experiment, 22 mL)
- For example, (5 × 10^5 cells per mL) × (V_1) = (0.35 × 10^5 cells per mL) × (22 mL), where V_1 = 1.54 mL of cell suspension

21. On the basis of the cell number calculation, remove V_1 mL of E8+20Y from 22 mL (that is, an equivalent volume to the volume of cell suspension needed for the experiment to achieve precise dilution). Then, add the calculated volume of cell suspension to the remaining E8+20Y. For example, if 1.54 mL of cell suspension is required, first remove 1.54 mL of E8+20Y from the 22 mL, leaving 20.46 mL. Then, add 1.54 mL of cell suspension to achieve a final cell concentration of 7.7 × 10^5 cells in 22 mL of E8+20Y.
    ▲ **CRITICAL STEP** Before transferring the calculated volume, pipette the single-cell suspension in the strainer tube from Step 18 to ensure thorough mixing and accurate cell numbers.
22. Gently invert several times or swirl the tube to mix the cell suspension evenly.
23. Pour the 22 mL cell suspension into a 25 mL reservoir.
24. Using a multichannel pipette with p200 regular tips, distribute 100 µL of cell suspension into each well of the 96-well U-bottom low-attachment plates.
    ▲ **CRITICAL STEP** When pipetting, do not scratch the interior of the wells with the tips.
25. Centrifuge the plates at 110*g* for 6 min at RT.
26. Incubate the plates in a 37 °C incubator with 5.0% CO_2 for 24 h.

Differentiation day (−1): dilution of Y solution

● **TIMING 15 min**

27. Prewarm 22 mL of fresh E8 Flex medium containing 100 µg/mL normocin (without Y, hereafter, E8) at RT.
28. Pour 22 mL of fresh E8 into a 25 mL reservoir.
29. Using a multichannel pipette with p200 regular tips, add 100 µL of E8 into each well, which brings the total volume to 200 µL per well.
    ▲ **CRITICAL STEP** Add slowly to keep the delicate pluripotent aggregates intact and to not disrupt the antiadherence coating present on the interior of the wells.
30. Incubate the plates in a 37 °C incubator with 5.0% CO_2 for 24 h.
31. Thaw 650 µL of Matrigel on ice overnight at 4 °C for the next day.

Differentiation day 0: transition to differentiation in E6 medium, inducing surface ectoderm by SB, BMP4 and low-bFGF treatment

● **TIMING 1 h 30 min**

▲ **CRITICAL** Perform all procedures on ice.

▲ **CRITICAL** The calculations for volumes in this treatment is standardized to a BMP concentration of 1.25 ng/mL (Fig. 4b), but the user should adjust this value appropriately for a large-scale differentiation at a different BMP concentration or multiple smaller concentration aliquots for treatments across a wide range of BMP concentrations in a titration experiment.

◆ **TROUBLESHOOTING**

32. Prepare E6 medium containing 2% Matrigel, 10 µM SB, 4 ng/mL bFGF, 1.25 ng/mL BMP4 and 100 µg/mL normocin. This medium will be referred to as E6SFB. E6SFB preparation is as follows:
    - Prepare 30 mL of E6 medium in a 50 mL conical tube and keep on ice. Ensure it is ice-cold before adding Matrigel
    - Remove 600 µL of E6 from the 30 mL and add 600 µL of Matrigel to achieve a 2% Matrigel concentration
      ▲ **CRITICAL STEP** Always perform this step first when preparing E6SFB to ensure accurate final concentrations of molecules added to the medium mixture.
    - Then, add 30 µL of 10 mM SB, 0.6 µL of 200 µg/mL bFGF, 3.75 µL of 10 µg/mL BMP4 (prepared by diluting a 100 µg/mL stock to 1:10) and 60 µL of 50 mg/mL normocin

to the E6 medium containing 2% Matrigel. Note, to prepare the 1:10 dilution of BMP4 (10 µg/mL), add 2 µL of 100 µg/mL BMP4 to 18 µL of E6 medium and mix thoroughly by pipetting

- Invert the tube several times to mix the E6SFB evenly, then keep on ice

▲ **CRITICAL STEP** The optimal concentration of BMP4 is cell line-dependent. We have found that for the WA25 cell line, a BMP4 concentration of 0.5 ng/mL works well. For most of the hiPS cell lines we have used, a concentration range of 0.75–2.00 ng/mL is typically recommended. We recommend performing BMP4 titration when using a new cell line (refer to Fig. 3 and Extended Data Fig. 1 for BMP4 titration data).

◆ **TROUBLESHOOTING**

33. Prepare 3 mL of E6 medium in a 15 mL conical tube to use for the washing step.
34. Collect all cell aggregates from the 96-well U-bottom low-attachment plates into a 2 mL round-bottom tube as follows:
    - Using p200 Wide-O tips and a multichannel pipette set to 170 µL (that is, ~30 µL less than the total volume of each well), carefully transfer all aggregates into a 100 mm Petri dish

      ▲ **CRITICAL STEP** Handle the pipette gently to avoid disrupting the integrity of the aggregates.
    - Gently swirl the Petri dish to gather all aggregates into the center of the dish
    - Using a p1000 Wide-O tip, transfer all aggregates from the Petri dish to a 2 mL round-bottom tube
35. Once the aggregates have settled at the bottom of the tube, carefully remove excess E8.
36. Wash the aggregates three times with 1 mL of E6 medium prepared in Step 33 to remove any remaining traces of E8.
37. After removing the final E6 wash, add 1 mL of E6SFB to the tube containing the aggregates.
38. Place a new 100 mm Petri dish on ice and add ~15 mL of the E6SFB prepared in Step 32.
39. Using a p1000 Wide-O tip, transfer all aggregates along with the 1 mL of E6SFB from the 2 mL round-bottom tube (from Step 37) into the Petri dish containing 15 mL of E6SFB on ice.
40. To ensure all aggregates are collected, rinse the 2 mL tube with an additional 1 mL of E6SFB and transfer this to the Petri dish.
41. Using a p200 Wide-O tip, transfer individual aggregates in 100 µL of E6SFB directly from the Petri dish into each well of a new 96-well U-bottom low-attachment plate. Add more E6SFB to the Petri dish as needed.
42. Incubate the plates in a 37 °C incubator with 5.0% CO_2 for 72 h.
43. Observe morphological changes daily.

Differentiation day 3: otic placode induction by LDN and bFGF treatment

● **TIMING 20 min**

▲ **CRITICAL** Samples are treated with LDN and FGF in a volume of 25 µl per well, resulting in a final volume of 125 µL in each well of the 96-well U-bottom low-attachment plates. Therefore, 5× LDN and FGF are prepared in the medium: 1 µM LDN (200 nM) and 250 ng/mL FGF (50 ng/mL). Note, parentheses '()' indicate the final concentrations of the molecules after treatment in a total volume of 125 µL.

44. Prepare E6 medium containing 100 µg/mL (1×) normocin, 1 µM LDN and 250 ng/mL bFGF (referred to as E6-5XLF):
    - Prepare 5 mL of E6 medium in a 15 mL conical tube and prewarm at RT
    - Add 10 µL of 50 mg/mL normocin, 0.5 µL of 10 mM LDN and 6.25 µL of 200 µg/mL bFGF
    - Invert the tube several times to mix evenly
45. Pour the 5 mL of E6-5XLF prepared in Step 44 into a 10 mL reservoir.
46. Using a multichannel pipette, add 25 µL of the E6-5XLF to each of the inner 60 wells in the 96-well U-bottom low-attachment plates. Note, wells on the edges of a 96-well plate are prone to evaporation, which can affect experimental accuracy.
47. Gently tap the plates on the surface of the biosafety cabinet to mix the medium.
48. Incubate the plates in a 37 °C incubator with 5.0% CO_2 for 72 h.
49. Observe morphological changes daily.

Differentiation day 6: nutrient supplementation

● **TIMING 15 min**

50. Prepare E6 medium containing 100 µg/mL normocin:
    - Prepare 11 mL of E6 medium in a 15 mL conical tube and prewarm at RT
    - Add 22 µL of 50 mg/mL normocin
    - Invert the tube several times to mix evenly
51. Pour the 11 mL of the medium prepared in Step 50 into a 10 mL reservoir.
52. Using a multichannel pipette, add 75 µL of fresh E6 to each of the inner 60 wells in the 96-well U-bottom low-attachment plates, bringing the final volume to 200 µL per well.
53. Gently tap the plates on the biosafety cabinet surface to mix the medium.
54. Incubate the plates in a 37 °C incubator with 5.0% CO_2 for 48 h.
55. Observe morphological changes daily.

Differentiation day 8: otic induction by CHIR treatment

● **TIMING 30 min**

▲ **CRITICAL** A total of 100 µL of spent medium will be removed, and 100 µL of medium containing CHIR will be added, resulting in a final concentration of 3 µM in a total volume of 200 µL per well. Therefore, prepare a 2× concentrated CHIR, which is 6 µM in the medium, and add it to each well.

56. Prepare E6 medium containing 100 µg/mL (1×) of normocin and 6 µM CHIR (referred to as E6-2XCH):
    - Prepare 15 mL of E6 medium in a 50 mL conical tube and prewarm at RT
    - Add 30 µL of 50 mg/mL normocin and 9 µL of 10 mM CHIR
    - Invert the tube several times to mix evenly
57. Using a multichannel pipette with p200 Wide-O tips, hold the pipette at a ~60° angle and carefully remove 100 µL of spent medium from the inner 60 wells of the 96-well U-bottom low-attachment plate, leaving 100 µL of the spent medium and the aggregates in each well.
    ▲ **CRITICAL STEP** Add slowly to keep the developing aggregates intact and to not disrupt the antiadherence coating present on the interior of the wells.
58. Pour the 15 mL of E6-2XCH prepared in Step 56 into a 25 mL reservoir.
59. Using a multichannel pipette with p200 regular tips, add 100 µL of fresh E6-2XCH to each well, bringing the final volume to 200 µL and final CHIR concentration to 3 µM.
60. Gently tap the plates on the biosafety cabinet surface to mix the medium.
61. Incubate the plates in a 37 °C incubator with 5.0% CO_2 for 48 h.
62. Observe morphological changes daily.

Differentiation day 10: continued otic vesicle induction by CHIR treatment

● **TIMING 30 min**

63. Prepare E6 medium containing 100 µg/mL (1×) of normocin and 3 µM (1×) CHIR (referred to as E6-1XCH):
    - Prepare 15 mL of E6 medium in a 50 mL conical tube and prewarm at RT
    - Add 30 µL of 50 mg/mL normocin and 4.5 µL of 10 mM CHIR
    - Invert the tube several times to mix evenly
64. Using a multichannel pipette with p200 Wide-O tips, hold the pipette at a ~60° angle and carefully remove 100 µL of spent medium from the inner 60 wells of the 96-well U-bottom low-attachment plate, leaving 100 µL of the spent medium and the aggregates in each well.
    ▲ **CRITICAL STEP** Add slowly to keep the developing aggregates intact and to not disrupt the antiadherence coating present on the interior of the wells
65. Pour the 15 mL of E6-1XCH prepared in Step 63 into a 25 mL reservoir.
66. Using a multichannel pipette with p200 regular tips, add 100 µL of fresh E6-1XCH to each well.
67. Gently tap the plates on the surface of the biosafety cabinet to mix the medium.
68. Incubate the plates in a 37 °C incubator with 5.0% CO_2 for 48 h.
69. Observe morphological changes daily.
70. On day 11, thaw 650 µL of Matrigel on ice overnight at 4 °C.
    ◆ **TROUBLESHOOTING**

Differentiation day 12: transition to floating culture in OMM with continued otic vesicle induction by CHIR treatment

● **TIMING 1 h 30 min**

▲ **CRITICAL** Using all aggregates from the inner 60 wells of two 96-well U-bottom plates (a total of 120 aggregates) will yield five 24-well low-attachment plates. The following medium preparation calculations reflect this amount; however, adjust the volumes as needed according to the number of aggregates being transferred to the 24-well low-attachment plates.

71. Prepare OMM containing 1% Matrigel, 3 µM CHIR and 100 µg/mL normocin. This medium will be referred to as OMM1%M-CH. OMM1%M-CH preparation is as follows:
    - Prepare 65 mL of OMM (see Table 5 for OMM composition) and keep on ice. Ensure it is ice-cold before adding Matrigel
    - Remove 650 µL of OMM from the 65 mL and add 650 µL of Matrigel to achieve 1% Matrigel concentration

      ▲ **CRITICAL STEP** Always perform this Matrigel addition step first, before introducing CHIR, to ensure that the final CHIR concentration is accurate.
    - Then, add 19.5 µL of 10 mM CHIR
    - Invert the OMM1%M-CH mixture several times to mix and keep on ice

      ◆ **TROUBLESHOOTING**
72. Place a 100 mm Petri dish on ice to chill until use.

    ◆ **TROUBLESHOOTING**
73. Collect all aggregates from 96-well U-bottom low-attachment plates to a 2 mL round-bottom tube as follows:
    - Using p200 Wide-O tips and a multichannel pipette set to 170 µL (that is, ~30 µL less than the total volume of each well), carefully transfer all aggregates into a 100 mm Petri dish at RT

      ▲ **CRITICAL STEP** Handle the pipette gently to avoid disrupting the integrity of the aggregates.
    - Gently swirl the Petri dish to gather all aggregates into the center of the dish
    - Using a p1000 Wide-O tip, transfer all aggregates from the Petri dish to a 2 mL round-bottom tube
74. Once the aggregates have settled at the bottom of the tube, carefully remove excess medium.
75. Wash the aggregates three times with 1 mL of Advanced DMEM/F12 medium.
76. After removing the final Advanced DMEM/F12 wash, add 1 mL of OMM1%M-CH prepared in Step 71 to the tube containing the aggregates and place on ice.
77. Pour ~15 mL of OMM1%M-CH into the chilled 100 mm Petri dish on ice (prepared in Step 72).
78. Using a p1000 Wide-O tip, transfer all aggregates that are in 1 mL of OMM1%M-CH from Step 76 into the Petri dish containing OMM1%M-CH on ice from Step 77.
79. Using a p1000 Wide-O tip, transfer each individual aggregate in 500 µL of OMM1%M-CH directly from the Petri dish into each well of 24-well low-attachment plates. Add additional OMM1%M-CH to the Petri dish as needed.
80. Gently swirl and tap the plates to ensure the surface of each well is covered with medium and the aggregates are neither attached to the bottom nor floating on the surface of the medium.
81. Incubate the plates on an orbital shaker at 65 rpm in a 37 °C incubator with 5.0% CO_2 for 72 h.
82. Observe morphological changes daily.
83. On day 14, thaw 320 µL of Matrigel on ice overnight at 4 °C.

    ◆ **TROUBLESHOOTING**

Differentiation day 15: half-medium change with OMM containing 1% Matrigel and continued otic vesicle induction

● **TIMING 30 min**

84. Prepare OMM1%M-CH:
    - Prepare 32 mL of OMM (refer to Table 5 for composition) in a 50 mL conical tube and keep on ice. Ensure it is ice-cold before adding Matrigel

- Remove 320 µL of OMM from the 32 mL and add 320 µL of Matrigel to achieve a final concentration of 1%
  ▲ **CRITICAL STEP** Always perform this Matrigel addition step first, before introducing CHIR, to ensure the final CHIR concentration is accurate.
- Then, add 9.6 µL of 10 mM CHIR
- Invert the tube containing OMM1%M-CH several times to mix evenly and keep on ice
  ◆ **TROUBLESHOOTING**

85. Using a p1000 regular tip, remove 250 µL of spent medium from each well of the 24-well plates, leaving ~250 µL of medium per well.
86. Add 250 µL of freshly prepared OMM1%M-CH into each well, bringing the final volume to ~500 µL per well.
87. Immediately and gently swirl to mix medium.
    ▲ **CRITICAL STEP** Confirm that all aggregates remain submerged and are not floating on the surface of the medium.
88. Incubate the plates on an orbital shaker at 65 rpm in a 37 °C incubator with 5.0% CO_2 for 72 h.
89. Observe morphological changes every 3 d.

Differentiation day 18: half-medium change for Matrigel dilution

● **TIMING 30 min**

90. Prewarm 32 mL of OMM without Matrigel or CHIR.
91. Remove 250 µL of spent medium from each well of the 24-well plates, leaving ~250 µL of medium per well.
92. Add 250 µL of fresh OMM into each well, bringing the final volume to ~500 µL per well.
93. Gently swirl the plates to evenly mix the medium.
    ▲ **CRITICAL STEP** Confirm that all aggregates remain submerged and are not floating on the surface of the medium.
94. Incubate the plates on an orbital shaker at 65 rpm in 37 °C incubator with 5.0% CO_2 for 72 h.
95. Starting from differentiation day 21, perform a full-medium change once per week by completely removing 500 µL of medium from each well and adding back 500 µL of fresh OMM. For experiments up to differentiation day 45, also perform two half-medium changes (that is, half-medium changes on Monday and Wednesday, followed by full-medium change on Friday). For experiments beyond differentiation day 45, perform full-medium changes every other day. In addition, adjust the total medium volume to 1–1.5 mL per well as needed, on the basis of organoid size (that is, larger), density (that is, denser and darker) and medium consumption rate (that is, color change to yellow) to ensure adequate nutrient supply.

Downstream assays

96. At designated time points, organoids can be dissociated or prepared for downstream analysis as described previously[11]. For cryoembedding, sectioning and immunostaining see Lee et al. 2022 (ref. 11); for whole-mount immunostaining with tissue clearing using the SHIELD method, follow option A; for vibratome sectioning for live-tissue analysis, follow option B; for vibratome sectioning for fixed-tissue analysis, follow option C[11]. Each method can be applicable at various differentiation stages, depending on the specific research question.
    - If following options A or C, organoids must first be fixed. For fixation, collect organoids with a Wide-O pipette tip or a cut pipette tip if a larger bore is needed, and transfer organoids from their original culture locations to a 2 mL round bottom Eppendorf. Aspirate the supernatann media and wash organoids with 1 mL 1× PBS three times. After aspirating the PBS the third time, add 1 mL 4% PFA and fix overnight in 4 °C cold room or fridge for ~12 h. After fixation, wash the organoids three times with 1× PBS and store indefinitely in PBS

(A) **SHIELD protocol—whole-mount staining**

● **TIMING 8 d**

▲ **CRITICAL** This protocol is adapted and optimized for organoid use on the basis of the method developed by Park et al. 2018 and Albanese et al. 2020 (refs. 86,87).

▲ **CRITICAL** Ensure that the organoids have been fixed in 4% PFA and then stored in 1× PBS after fixation.

▲ **CRITICAL** Verify the availability of primary and secondary antibodies in advance to ensure sufficient quantities for the protocol. It is highly recommended to verify that antibodies are effective in cryosections using immunohistochemistry before beginning whole-mount staining to avoid wasting samples.

(i) Day 1: tissue adaptation in SHIELD-OFF Solution.

● **(TIMING 15 min): prepare 20 mL of 12.5% SHIELD-Epoxy-OFF solution on ice.**

- In a 50 mL conical tube, add 5 mL of SHIELD Buffer to 12.5 mL of deionized (DI) water
- Vortex thoroughly to mix and place the tube on ice
- Add 2.5 mL SHIELD-Epoxy to the solution, bringing the total volume to 20 mL
- Vortex again to mix the solution thoroughly

(ii) Incubate the the organoids in ice-cold 12.5% SHIELD-Epoxy-OFF solution in 2 mL round-bottom tubes. Note, use one 2 mL round-bottom tube for one-to-three organoids (~3 mm each), depending on size. For larger (>4.5 mm) or more fragile organoids, place only one organoid per tube

- Carefully transfer the organoids to 2 mL round-bottom tubes using a cut Wide-O tip or a scooper

  ▲ **CRITICAL STEP** Handle the organoids gently to maintain their integrity.
- Carefully remove any residual solution from the tubes
- Gently add 1.5 mL of the 12.5% SHIELD-Epoxy-OFF solution prepared in Step 96A(i) to each tube. Note, the remaining 12.5% SHIELD-Epoxy-OFF can be stored at 4 °C up to 2 weeks

  ▲ **CRITICAL STEP** If preserving the endogenous fluorescence in the organoids, keep the tubes covered with aluminum foil or store them in a light-blocking container.

(iii) Incubate for 48 h at 4 °C. (optional: place the tubes on a gentle shaker or rotator for even exposure to the solution).

(iv) Day 3: transition to SHIELD-ON solution.

● **(TIMING 10 min): set the oven temperature to 37 °C.**

(v) Prewarm the SHIELD-ON solution in the oven at 37 °C.

(vi) Carefully remove the 12.5% SHIELD-Epoxy-OFF solution from each tube containing organoids.

(vii) Gently add 1.5 mL of SHIELD-ON solution to each tube.

(viii) Incubate the tubes for 24 h in the oven at 37 °C (optional: place the tubes on a rotator).

(ix) Day 4: transition to delipidation buffer.

● **(TIMING 3.5 h): carefully remove the SHIELD-ON solution from each tube containing the organoids.**

(x) Wash the organoids in 1.5 mL of 1× PBS on a gentle shaker at RT for 3 h, replenishing the 1× PBS every 30 min.

(xi) (Optional) If not using the commercially available delipidation buffer from LifeCanvas, prepare an SDS clearing solution near the last hour of the 1× PBS washing step. The SDS clearing solution consists of 200 mM SDS, 10 mM sodium borate and 100 mM sodium sulfite, with a pH of 9.0. To prepare 100 mL of SDS clearing solution:

- Set an oven to 55 °C
- Add 100 mL of DI water to a glass bottle containing a magnetic stir bar, and mark the water level on the bottle
- Pour out approximately half of the water (~50 mL), leaving the other half (~50 mL) in the bottle with the stir bar
- Place the bottle on a hot plate with heating and stirring functions
- With stirring on, gradually add 5.77 g of SDS (molecular weight, (MW): 288.38 g/mol), 0.38 g of sodium borate (MW: 381.37 g/mol)

and 1.26 g of sodium sulfite (MW: 126.04 g/mol), stirring thoroughly after each addition. Note, setting the hot plate to 50–55 °C may be necessary to dissolve the SDS fully. However, once the SDS is fully dissolved, reduce the temperature to 30 °C before adding sodium borate and sodium sulfite to maintain their stability

- Once all components are dissolved, add DI water to bring the total volume back to 100 mL, using the previously marked level on the bottle as a guide
- Adjust the pH to 9.0 by adding 5 M NaOH in small drops with a p200 pipette while continuously stirring. Note, adding NaOH gradually and stirring thoroughly ensures an accurate pH adjustment. Any remaining SDS clearing solution can be stored at RT

(xii) Carefully remove the final 1× PBS wash solution, and add 1 mL of delipidation buffer (or SDS clearing solution) to each tube.

(xiii) Incubate the tubes overnight in 55 °C (optional: use a gentle shaker or rotator). Note, according to LifeCanvas, delipidation can take anywhere from 6 h to 48 h, depending on the sample size and composition. This step should make the sample more translucent but not fully clear. The standard protocol for cerebral organoids is 48 h, while 12–18 h (overnight) is sufficient for skin and IEOs.

(xiv) Day 5: incubation with primary antibodies.

● (TIMING 6.5 h): carefully remove the delipidation buffer (or SDS clearing solution) from the tubes containing the organoids.

(xv) Wash organoids thoroughly with 1mL of 1× PBS containing 0.1% Triton X-100 (referred to as 0.1% PBS-T) on a gentle shaker at RT for a total of 6 h. Replenish the 0.1% PBS-T every hour for the first 3 h of the washing process.

(xvi) Prepare the primary antibody solutions at the concentrations recommended in Table 2 in 0.1% PBS-T. If other antibodies are used, 10 µg/mL is a good starting point. The total volume needed will vary depending on the sizes and number of organoids per tube. Ensure that the solution fully covers the entire sample(s) in the tube, enabling gentle shaking without inversion. Typically, 100–500 µL of antibody solution is sufficient, depending on sample size and requirements. Note, verify the antibody stock concentrations on each vial or manufacturers' websites before use.

- Equation: $C_1V_1 = C_2V_2$
  - (Stock antibody concentration) × (volume of stock antibody needed) = (desired concentration) × (final solution volume)

(xvii) Carefully remove the final 0.1% PBS-T wash from the sample tube.

(xviii) Add 100 µL to 500 µL of the prepared antibody solution from Step 96A(xvi) into the sample tube.

(xix) Incubate the tubes with samples overnight on a gentle shaker at RT. Note, avoid inverting or rotating the tubes if the antibody solution volume is low (<500 µL) or the samples are fragile. If the antibody solution volume is over 1 mL (or >500 µL) per tube, gentle inversion or rotation may be performed during incubation. However, ensure that the samples move freely within the solution without getting trapped under the tube lid.

(xx) Day 6: incubation with secondary antibodies.

● (TIMING 4.5 h): carefully remove the primary antibody solution from the sample tubes.

(xxi) Wash organoids thoroughly with 1 mL of 0.1% PBS-T on a gentle shaker at RT for a total of 4 h. Replenish the 0.1% PBS-T every hour throughout the 4 h washing process.

(xxii) Prepare the secondary antibody solutions by adding each antibody at the dilutions listed in Table 2 in 0.1% PBS-T. Similar to that for primary antibodies, unless listed, a concentration of 10 µg/mL is appropriate for secondary staining. A total of 1 mL per tube should be sufficient.

▲ **CAUTION** The secondary antibodies are light-sensitive. Ensure that samples remain protected from light.

(xxiii) Carefully remove the final 0.1% PBS-T wash from each sample tube.

(xxiv) Add 1 mL of the prepared secondary antibody solution from Step 96A(xxii) into each sample tube.

(xxv) Incubate overnight at RT on a gentle shaker, positioning the tubes at a slight angle to encourage gentle circulation of the solution.
▲ **CAUTION** The secondary antibodies are light-sensitive. Cover the tubes with aluminum foil or place them in a dark box to protect from light while on the gentle shaker.

(xxvi) Day 7: index matching (clearing).
● **(TIMING 7.5 h): carefully remove secondary antibody solutions from each sample tubes.**

(xxvii) Wash organoids thoroughly with 1 mL of 0.1% PBS-T on a gentle shaker at RT for a total of 4 h, replenishing the 0.1% PBS-T every hour throughout the 4 h washing process.

(xxviii) While washing, prepare a half-step Easy-Index Matching Medium by combining 1× PBS and Easy-Index Solution (from the SHIELD Kit) in a 1:1 ratio. Prepare enough for 1 mL per tube. Note, Easy-Index Solution is highly viscous and may cause the organoids to collapse if pipetted too quickly. Depending on the organoid size and fragility, this step should begin with a lower concentration of Easy-Index Solution, which then can be increased in concentration. For example, prepare a series of dilutions of increasing concentration starting from 30%.

(xxix) Remove the final 0.1% PBS-T wash and gently add 1 mL of the prepared half-step Easy-Index Matching Medium to each tube.

(xxx) Incubate the tubes in a 37 °C oven for 3 h (optional: gentle rotation).

(xxxi) Carefully remove the half-step Easy-Index Matching Medium from the sample tubes.

(xxxii) Slowly add 1–1.5 mL of 100% Easy-Index Solution to each tube by gently pipetting the solution along the tube wall to avoid disturbing the organoids. Note: if a lower concentration of Easy-Index Solution was used previously, adjust the solution accordingly, and repeat Steps 96A(xxxi) and 96A(xxxii), increasing the concentration until 100% Easy-Index Solution is reached.

(xxxiii) Seal the tube caps by parafilm to prevent evaporation and leakage.

(xxxiv) Incubate the tubes on a gentle rotator in a 37 °C oven overnight.

(xxxv) Day 8: mounting samples.
● **(TIMING 30 min): prepare double-sided adhesive silicone spacers by cutting the required amount to mount samples (Fig. 4a in Lee et al. 2022)[11].**

(xxxvi) Peel one side of the silicone spacer and adhere it to a coverslip. Press gently to avoid cracking the coverslip.

(xxxvii) Remove the remaining side of the silicone adhesive backing.

(xxxviii) Cut a p1000 pipette tip to fit the size of the organoids. Carefully pipette each organoid in 100% Easy-Index Solution and place it into each well of the silicone spacer.

(xxxix) Fill the remaining space in each well with additional 100% Easy-Index Solution. Ensure that the liquid is slightly raised above the silicone spacer when viewed from the side to prevent air bubbles during mounting.

(xl) Gently place another coverslip on top, aligning it from one edge to another. Note: if bubbles form, gently lift one edge and add more 100% Easy-Index Solution with a pipette. A 12CIR circular coverslip is useful for mounting individual organoids separately on the silicone spacer, particularly if the sample may need to be retrieved and restained. After this step (Step 96A(xl)), samples can be cautiously imaged from one side for a preliminary view, until Step 96A(xlii) is completed, which enables stable imaging from both sides.
▲ **CAUTION** Do not press on this coverslip.

(xli) Apply clear nail polish along the edges of one side of the silicon isolator cassette and let it to dry completely.

(xlii) Repeat Step 96A(xli) on the opposite side of the silicon isolator cassette. Note, samples can now be imaged stably from both sides using a confocal microscope such as a Nikon Ti2 or A1R. Large, tiled images with large z-stacks are preferred for this orientation. That being said, clearing also enables the imaging of interior structures with high resolution for additional investigation.

(xliii) Store the whole-mount-stained samples at 4 °C in a light-protected box until imaging. Note, fluorophore signals have been verified to remain stable for at least 2 months and beyond in the Koehler lab. For optimal long-term signal preservation, transfer the stained organoids to a 2 mL round-bottom tube containing Easy-Index Solution, seal the tubes and store them in the dark environment (see Fig. 6 for examples of samples maintained for over 2 years without apparent signal degradation).

(B) **Live-organoid vibratome sectioning protocol**

● **TIMING 2 h**

▲ **CRITICAL** Perform all steps involving live organoid tissue on ice. Ensure that all materials and instruments are prepared before beginning the procedure.

(i) Calibrate and prepare vibratome (Leica): follow the instruction manual, which includes a vibro-check for calibration and ensuring the vibratome is ice-cold during the sectioning procedure.

(ii) Sample preparation: prepare 2% LMPA by dissolving 4 g of LMPA powder in 100 mL of double-distilled water in a heat-resistant Schott Glass bottle with a stir bar.

(iii) Microwave the LMPA in 10–15 s pulses, swirling intermittently until the powder is fully dissolved and just begins to boil.

▲ **CAUTION** Dissolved LMPA is extremely hot and can cause burns; handle with care.

(iv) Keep the dissolved LMPA on a hot plate set to 41 °C with stirring at 75 rpm to cool and keep in liquid form.

(v) Once the LMPA has cooled to 41 °C, retrieve the organoids from the incubator and wash them three times in 1× DPBS in a 2 mL round bottom tube.

(vi) Transfer the organoids to cryomolds using a cut Wide-O p1000 pipette tip.

(vii) Carefully remove the excess 1× DPBS using a p200 pipette or a syringe fitted with a blunt-end needle.

(viii) Add the cooled, liquid LMPA to the cryomold to cover the organoids completely. Arrange tissues briefly with a sterile wooden dowel or pipette tip if necessary.

(ix) Place the cryomold containing the organoids on ice, ensuring it sits horizontally to allow LMPA to solidify without shifting tissues.

(x) Prepare a 12-well plate filled with ice-cold 1× DBPS for section collection.

(xi) Once the LMPA has fully set (it will appear slightly blue and cloudy), carefully remove the LMPA block with the embedded organoids from the mold. Blot gently with a Kimwipe to remove any excess moisture.

(xii) Vibratome sectioning: apply superglue to the mold holder of a metal buffer tray, then invert the LMPA block onto the mold holder with the organoids facing upwards. Allow the glue to set fully before proceeding.

(xiii) Place the metal buffer tray with the LMPA block in the vibratome chamber, and align the front edge parallel to the sapphire vibratome blade.

(xiv) Fill the metal buffer tray with ice-cold sterile 1× DPBS until it reaches the top surface of the LMPA block and add ice to the outer tray.

(xv) Lower the sapphire vibratome blade until it just approaches the 1× DPBS surface.

(xvi) Set the start (front) and end (back) positions of the blade movement.

(xvii) Retract the sapphire vibratome blade and continue lowering until it touches the 1× DPBS surface.

(xviii) With a speed of 4 and a frequency of 4, section the organoid tissues at 200–250 µm thickness per slice. Note: if tissues dislodge prematurely from the LMPA block, consider increasing the agarose concentration up to 4%.

(xix) Carefully collect each slice with a large, flat metal spoon as it floats off and transfer it to a 12-well plate filled with ice-cold 1× DPBS from Step 96B(x).

(xx) Continue collecting sections, refilling ice as needed.

(xxi) Transfer the 12-well plate to a biosafety cabinet.

(xxii) Prepare prewarmed OMM in a 100 mm Petri dish.

(xxiii) Transfer tissue slices to the prewarmed OMM.

(xxiv) Gently dislodge the tissues from the agarose with a pair of sterile forceps.
(xxv) Transfer the dislodged tissue slices to a 12-well culture plate or a 12-well glass-bottom plate in OMM for recovery, short-term culture or further processing (for example, imaging).
(xxvi) (Optional step; recommended for long-term culture) To prevent the respherification of the tissue slices, pin the sliced tissues under Minutien pins adhered to 18-mm round coverslips with a small drop of Sylgard. Transfer pinned tissues to a new sterile 6- or 12-well plate for long-term culture.
(xxvii) Incubate tissues in a 37 °C incubator with 5% CO_2 and proceed with downstream experiments as required and described in the 'Experimental design' section.

(C) **Fixed-organoid vibratome sectioning protocol**

● **TIMING 2 h**

▲ **CRITICAL** Use organoids that have been fixed overnight in 4% PFA or stored in 1× DPBS at 4 °C after fixation. Fixed-organoids do not require ice-cold 1× DPBS; RT 1× DPBS is sufficient.

(i) Similar to the live-organoid vibratome sectioning protocol (Step 96B), calibrate and prepare the vibratome according to manufacturer's instructions. This procedure should be performed on a vibratome designated for fixed tissue.
(ii) Follow Steps 96B(ii–xviii) (excluding Step 96B(v)) in the live-organoid vibratome sectioning protocol, adjusting the section thickness to 120–150 µm.
(iii) As tissue slices float off during vibratome sectioning, collect each slice using a large, flat metal spoon and transfer it to a 100 mm Petri dish filled with 1× DPBS.
(iv) Using a pair of sterile forceps, carefully dislodge the samples from the agarose.
(v) Transfer the dislodged slices to a 12-well glass-bottom plates in 1× DPBS for whole-mount staining, immunostaining and imaging, using standard reagents and procedures as described in the downstream assays in our earlier protocol: Step 141A (single-cell capture) and Step 141B (sample preparation, cryoembedding, cryosectioning and immunostaining)[11].

Troubleshooting

General troubleshooting guidelines for sensory organoid differentiation are available in our previous *Nature Protocols* publication on the differentiation of SKOs from hiPS cells[11]. Below, we provide additional troubleshooting advice tailored specifically for generating IEO models:

BMP4 titration on day 0 to evaluate new cell lines (Step 32)

As described before, optimal BMP4 concentration is not only cell line dependent, as endogenous BMP4 levels can vary across cell lines and are also influenced by the specific BMP4 product used. The values provided here are based on PeproTech BMP4. For the best results, perform a BMP4 titration when introducing a new cell line. Test 3–4 different BMP4 concentrations and monitor cultures through day 12 of differentiation to evaluate success (Fig. 3). For reference, we found that 0.5–0.75 ng/mL of BMP4 is optimal for WA25 hES cells, while a slightly higher and broader range of 0.75–2.00 ng/mL has worked well for WTC-11 hiPS cells in our previous studies[28,29,31] (Fig. 4b). LUMC04i10 and LUMC44i44 displayed optimal induction at a Peprotech BMP4 concentration of 1.25 ng/ml in our previous studies[28] (van der Valk et al. *Cell Reports* 2023, Fig. 1e). We anticipate that a range of 0.5–2.5 ng/mL will be suitable for most PS cell lines.

Working with Matrigel (Steps 31–32, 70–72 and 83–84)

Matrigel is a temperature-sensitive extracellular matrix derived from mouse sarcomas that supports aggregate cultures by promoting structural organization and cell proliferation. Because it begins to gel above 16 °C, Matrigel should always be stored frozen and thawed overnight on ice before use. All media, pipette tips and labware that come into contact with

Matrigel should be prechilled to 4 °C to prevent premature gelling and ensure even distribution. A poor dilution of Matrigel in the medium can lead to visible clumping under phase-contrast microscopy, especially around cell aggregates, and may cause cells to migrate away from the aggregate into dense Matrigel regions. To avoid this, mix Matrigel gently but thoroughly into a cold medium using chilled pipette tips, avoiding bubbles, and remix the solution if uneven distribution is observed.

Timing

Steps 1–95, differentiation:
Total time to observe otic vesicle formation: ~10 d
Total time to generate sensory epithelium with hair cells: ~35 d onward
Steps 1–26 (day −2), cell dissociation and aggregation: 50 min
Steps 27–31 (day −1), dilution of Y solution: 15 min
Steps 32–43 (day 0), transition to differentiation in E6SFB: 1 h 30 min
Steps 44–49 (day 3), LDN and bFGF treatment: 20 min
Steps 50–55 (day 6), nutrient supplementation: 15 min
Steps 56–62 (day 8), CHIR treatment: 30 min
Steps 63–70 (day 10), CHIR treatment: 30 min
Steps 71–83 (day 12), transition to floating culture in OMM1%M-CH: 1 h 30 min
Steps 84–89 (day 15), half-medium change with OMM1%M-CH: 30 min
Steps 90–95 (day 18 onward), half-medium change with OMM: 30 min
Step 96, downstream assays:
Step 96A(i–xliii), whole-mount staining with SHIELD tissue clearing method: 8 d
Step 96B(i–xxvii), live-organoid vibratome sectioning: 2 h
Step 96C(i–v), fixed-organoid vibratome sectioning: 2 h

Anticipated results

Table 1 outlines key checkpoints for evaluating IEO differentiation efficiency, along with expected outcomes at each stage. When the differentiation experiment is conducted accurately, IEOs will progress through distinct developmental stages, observable with an inverted microscope (Figs. 2–4 and Extended Data Fig. 1).

During days 0–3 of differentiation, the formation of an epithelium on the aggregate's surface will indicate the initial differentiation of the organoids in response to the integrin and laminin signals from extracellular matrix proteins present in Matrigel and exogenous morphogens delivered in the media (Fig. 2). Using the optimal BMP4 concentration on day 0, specific to the cell line and BMP4 vendor, this epithelium will develop into surface ectoderm by day 3, and in response to bFGF and LDN, into placodal ectoderm by day 6 to day 8 (Fig. 3 and Extended Data Fig. 1). These cell aggregates will form bulging otic placodes between day 10 and day 12, with vesicle-like structures emerging by day 18, visible under brightfield or phase-contrast microscopy (Fig. 3 and Extended Data Figs. 1 and 2).

Over the following week, these vesicles should differentiate further, exhibiting epithelial cells surrounded by mesenchymal cells. By day 21, the organoids should display clear morphological features of otic vesicles, characterized by a distinct epithelial layer with an inner lumen (Fig. 4c,d). Between days 25 and 35, the organoids will begin developing sensory patches resembling those in native vestibular organs, with hair cell progenitors identifiable through specific markers, such as PCP4, POU4F3 and MYO7A, as early as day 36 (Fig. 5a). These IEOs will be immediately surrounded by a layer of $OTOR^{+}$ periotic mesenchyme (Fig. 5b).

The sensory patches will further differentiate into hair cells, featuring stereocilia bundles, identifiable by phalloidin staining for actin by around day 50 (Fig. 5f). $SOX2^{+}$ supporting cells

will also be present, contributing to the structural organization of the sensory epithelium as the organoid continues to mature (Fig. 5a). As the innervation of TUBB3$^+$ complex neuronal network to hair cells is observed (Figs. 5f,g and 6), synaptic connections between hair cells and neurons can be confirmed through immunostaining for synaptic markers and electron microscopy[28]. During the period from days 50 to 110, the organoids will continue to mature, showing increased hair cell and supporting cell numbers and complexity[28]. Functional assessments, such as electrophysiological recordings[30,45], may demonstrate functional capabilities in hair cells.

By day 75, the organoids are expected to exhibit a structure and cellular composition resembling the native second-trimester inner ear, including distinctly vestibular sensory epithelia and supporting structures (Figs. 4d and 5a,e). While development and maturation timeline may vary slightly depending on the cell lines used, this standardized protocol is anticipated to yield the desired morphology and functionality in over 80% of IEOs.

Beyond day 100, IEOs may begin to show signs of overgrowth or structural disorganization, including excessive proliferation of certain cell types, which can obscure the location of IEO sensory epithelia. Therefore, we recommend using the organoids for downstream analyses before day ~150 to ensure optimal quality and relevance. This IEO model is expected to serve as a robust tool for studying the human inner ear development, mechanisms of hearing and balance loss and potential therapeutic interventions.

Data availability

All data supporting the findings of this study are available via https://koehler-lab.org/resources. The Github repository is available via GitHub at https://github.com/Koehler-Lab. The gEAR Inner Ear Organoid Developmental Atlas is available via https://umgear.org/p?l=InnerEarOrganoidAtlas. The gEAR data from van der Valk. et al. *Cell Reports*, 2023 is available via https://umgear.org/p?l=hIEOandInnerEar.

Received: 7 August 2024; Accepted: 1 April 2025;
Published online: 02 June 2025

References

1. World Health Organization. Deafness and hearing loss. *WHO* https://www.who.int/news-room/fact-sheets/detail/deafness-and-hearing-loss (26 Feb 2025)
2. Lv, J. et al. AAV1-hOTOF gene therapy for autosomal recessive deafness 9: a single-arm trial. *Lancet* **403**, 2317–2325 (2024).
3. Qi, J. et al. AAV-mediated gene therapy restores hearing in patients with DFNB9 deafness. *Adv. Sci.* **11**, 2306788 (2024).
4. Wang, H. et al. Bilateral gene therapy in children with autosomal recessive deafness 9: single-arm trial results. *Nat. Med.* https://doi.org/10.1038/s41591-024-03023-5 (2024).
5. Loewa, A., Feng, J. J. & Hedtrich, S. Human disease models in drug development. *Nat. Rev. Bioeng.* **1**, 545–559 (2023).
6. Agrawal, Y., Ward, B. K. & Minor, L. B. Vestibular dysfunction: prevalence, impact and need for targeted treatment. *J. Vestib. Res.* **23**, 113–117 (2013).
7. Eppsteiner, R. W. & Smith, R. J. H. Genetic disorders of the vestibular system. *Curr. Opin. Otolaryngol. Head. Neck Surg.* **19**, 397–402 (2011).
8. Lahlou, H., Zhu, H., Zhou, W. & Edge, A. S. B. Pharmacological regeneration of sensory hair cells restores afferent innervation and vestibular function. *J. Clin. Investig.* https://doi.org/10.1172/jci181201 (2024).
9. Nist-Lund, C., Kim, J. & Koehler, K. R. Advancements in inner ear development, regeneration, and repair through otic organoids. *Curr. Opin. Genet. Dev.* **76**, 101954 (2022).
10. Wang, T. et al. Single-cell transcriptomic atlas reveals increased regeneration in diseased human inner ear balance organs. *Nat. Commun.* **15**, 4833 (2024).
11. Lee, J. et al. Generation and characterization of hair-bearing skin organoids from human pluripotent stem cells. *Nat. Protoc.* **17**, 1266–1305 (2022).
12. Lee, J. et al. Hair-bearing human skin generated entirely from pluripotent stem cells. *Nature* **582**, 399–404 (2020).
13. Roccio, M. & Edge, A. S. B. Inner ear organoids: new tools to understand neurosensory cell development, degeneration and regeneration. *Development* **146**, dev177188 (2019).
14. Tang, P.-C., Hashino, E. & Nelson, R. F. Progress in modeling and targeting inner ear disorders with pluripotent stem cells. *Stem Cell Rep.* **14**, 996–1008 (2020).
15. van der Valk, W. H., Steinhart, M. R., Zhang, J. & Koehler, K. R. Building inner ears: recent advances and future challenges for in vitro organoid systems. *Cell Death Differ.* **28**, 24–34 (2021).
16. Kim, J., Koo, B.-K. & Knoblich, J. A. Human organoids: model systems for human biology and medicine. *Nat. Rev. Mol. Cell Biol.* **21**, 571–584 (2020).
17. Zhao, Z. et al. Organoids. *Nat. Rev. Methods Prim.* **2**, 94 (2022).
18. Sasai, Y. Cytosystems dynamics in self-organization of tissue architecture. *Nature* **493**, 318–326 (2013).
19. Locher, H. et al. Neurosensory development and cell fate determination in the human cochlea. *Neural Dev.* **8**, 20 (2013).
20. Locher, H. et al. Development of the stria vascularis and potassium regulation in the human fetal cochlea: insights into hereditary sensorineural hearing loss. *Dev. Neurobiol.* **75**, 1219–1240 (2015).
21. Beelen, E. S. A. van et al. Migration and fate of vestibular melanocytes during development of the human inner ear. *Dev. Neurobiol.* https://doi.org/10.1002/dneu.22786 (2020).
22. Yang, L. M. & Ornitz, D. M. Sculpting the skull through neurosensory epithelial–mesenchymal signaling. *Dev. Dyn.* **248**, 88–97 (2019).
23. Groves, A. K. & Bronner-Fraser, M. Competence, specification and commitment in otic placode induction. *Development* **127**, 3489–3499 (2000).
24. Groves, A. K. & Fekete, D. M. Shaping sound in space: the regulation of inner ear patterning. *Development* **139**, 245–257 (2011).
25. Fekete, D. M. & Wu, D. K. Revisiting cell fate specification in the inner ear. *Curr. Opin. Neurobiol.* **12**, 35–42 (2002).
26. Oshima, K. et al. Mechanosensitive hair cell-like cells from embryonic and induced pluripotent stem cells. *Cell* **141**, 704–716 (2010).
27. Ronaghi, M. et al. Inner ear hair cell-like cells from human embryonic stem cells. *Stem Cells Dev.* **23**, 1275–1284 (2014).
28. van der Valk, W. H. et al. A single-cell level comparison of human inner ear organoids with the human cochlea and vestibular organs. *Cell Rep.* **42**, 112623 (2023).
29. Steinhart, M. R. et al. Mapping oto-pharyngeal development in a human inner ear organoid model. *Development* **150**, dev201871 (2023).

30. Koehler, K. R. et al. Generation of inner ear organoids containing functional hair cells from human pluripotent stem cells. *Nat. Biotechnol.* **35**, 583–589 (2017).
31. Doda, D. et al. Human pluripotent stem cells-derived inner ear organoids recapitulate otic development in vitro. *Development* **150**, dev201865 (2023).
32. Watanabe, K. et al. Directed differentiation of telencephalic precursors from embryonic stem cells. *Nat. Neurosci.* **8**, 288–296 (2005).
33. Sasai, Y., Eiraku, M. & Suga, H. In vitro organogenesis in three dimensions: self-organising stem cells. *Development* **139**, 4111–4121 (2012).
34. Kadoshima, T. et al. Self-organization of axial polarity, inside-out layer pattern, and species-specific progenitor dynamics in human ES cell-derived neocortex. *Proc. Natl Acad. Sci. USA* **110**, 20284–20289 (2013).
35. Eiraku, M. et al. Self-organizing optic-cup morphogenesis in three-dimensional culture. *Nature* **472**, 51–56 (2011).
36. Eiraku, M. et al. Self-organized formation of polarized cortical tissues from ESCs and its active manipulation by extrinsic signals. *Cell Stem Cell* **3**, 519–532 (2008).
37. Nakano, T. et al. Self-formation of optic cups and storable stratified neural retina from human ESCs. *Cell Stem Cell* **10**, 771–785 (2012).
38. Suga, H. et al. Self-formation of functional adenohypophysis in three-dimensional culture. *Nature* **480**, 57–62 (2011).
39. Muguruma, K. et al. Ontogeny-recapitulating generation and tissue integration of ES cell-derived Purkinje cells. *Nat. Neurosci.* **13**, 1171–1180 (2010).
40. Koehler, K. R. & Hashino, E. 3D mouse embryonic stem cell culture for generating inner ear organoids. *Nat. Protoc.* **9**, 1229–1244 (2014).
41. Koehler, K. R., Mikosz, A. M., Molosh, A. I., Patel, D. & Hashino, E. Generation of inner ear sensory epithelia from pluripotent stem cells in 3D culture. *Nature* **500**, 217–221 (2013).
42. Lippmann, E. S., Estevez-Silva, M. C. & Ashton, R. S. Defined human pluripotent stem cell culture enables highly efficient neuroepithelium derivation without small molecule inhibitors. *Stem Cells* **32**, 1032–1042 (2014).
43. Tchieu, J. et al. A modular platform for differentiation of human PSCs into all major ectodermal lineages. *Cell Stem Cell* **21**, 399–410.e7 (2017).
44. Ueda, Y., Moore, S. T. & Hashino, E. Embryonic stem cell protocols. *Methods Mol. Biol.* **2520**, 135–150 (2021).
45. Moore, S. T. et al. Generating high-fidelity cochlear organoids from human pluripotent stem cells. *Cell Stem Cell* **30**, 950–961.e7 (2023).
46. Nie, J. & Hashino, E. Generation of inner ear organoids from human pluripotent stem cells. *Methods Cell Biol.* **159**, 303–321 (2020).
47. Jeong, M. et al. Generating inner ear organoids containing putative cochlear hair cells from human pluripotent stem cells. *Cell Death Dis.* **9**, 922 (2018).
48. Matsuoka, A. J. et al. Directed differentiation of human embryonic stem cells toward placode-derived spiral ganglion-like sensory neurons. *Stem Cells Transl. Med.* **6**, 923–936 (2016).
49. Hartman, B. H. et al. Fbxo2VHC mouse and embryonic stem cell reporter lines delineate in vitro-generated inner ear sensory epithelia cells and enable otic lineage selection and Cre-recombination. *Dev. Biol.* **443**, 64–77 (2018).
50. Schaefer, S. A. et al. From Otic induction to hair cell production: Pax2 EGFP cell line illuminates key stages of development in mouse inner ear organoid model. *Stem Cells Dev.* **27**, 237–251 (2018).
51. Lancaster, M. A. & Knoblich, J. A. Organogenesis in a dish: modeling development and disease using organoid technologies. *Science* **345**, 1247125 (2014).
52. Paşca, S. P. Assembling human brain organoids. *Science* **363**, 126–127 (2019).
53. Ohlemiller, K. K., Jones, S. M. & Johnson, K. R. Application of mouse models to research in hearing and balance. *J. Assoc. Res. Otolaryngol.* **17**, 493–523 (2016).
54. Carlson, R. J. & Avraham, K. B. Emerging complexities of the mouse as a model for human hearing loss. *Proc. Natl Acad. Sci. USA* **119**, e2211351119 (2022).
55. Roccio, M. et al. Molecular characterization and prospective isolation of human fetal cochlear hair cell progenitors. *Nat. Commun.* **9**, 4027 (2018).
56. Beelen, E. S. Avan et al. Efficient viral transduction in fetal and adult human inner ear explants with AAV9-PHP.B vectors. *Biomolecules* **12**, 816 (2022).
57. Bok, J. et al. Opposing gradients of Gli repressor and activators mediate Shh signaling along the dorsoventral axis of the inner ear. *Development* **134**, 1713–1722 (2007).
58. Riccomagno, M. M., Martinu, L., Mulheisen, M., Wu, D. K. & Epstein, D. J. Specification of the mammalian cochlea is dependent on Sonic hedgehog. *Gene Dev.* **16**, 2365–2378 (2002).
59. Brown, A. S. & Epstein, D. J. Otic ablation of smoothened reveals direct and indirect requirements for Hedgehog signaling in inner ear development. *Development* **138**, 3967–3976 (2011).
60. Brown, A. S., Rakowiecki, S. M., Li, J. Y. H. & Epstein, D. J. The cochlear sensory epithelium derives from Wnt responsive cells in the dorsomedial otic cup. *Dev. Biol.* **399**, 177–187 (2015).
61. Riccomagno, M. M., Takada, S. & Epstein, D. J. Wnt-dependent regulation of inner ear morphogenesis is balanced by the opposing and supporting roles of Shh. *Gene Dev.* **19**, 1612–1623 (2005).
62. Schlosser, G. Induction and specification of cranial placodes. *Dev. Biol.* **294**, 303–351 (2006).
63. Barald, K. F. & Kelley, M. W. From placode to polarization: new tunes in inner ear development. *Development* **131**, 4119–4130 (2004).
64. Munnamalai, V. & Fekete, D. M. Building the human inner ear in an organoid. *Nat. Biotechnol.* **35**, 518–520 (2017).
65. Maier, E. C., Saxena, A., Alsina, B., Bronner, M. E. & Whitfield, T. T. Sensational placodes: neurogenesis in the otic and olfactory systems. *Dev. Biol.* **389**, 50–67 (2014).
66. Ueda, Y. et al. Defining developmental trajectories of prosensory cells in human inner ear organoids at single-cell resolution. *Development* **150**, dev201071 (2023).
67. Nie, J., Ueda, Y., Solivais, A. J. & Hashino, E. CHD7 regulates otic lineage specification and hair cell differentiation in human inner ear organoids. *Nat. Commun.* **13**, 7053 (2022).
68. Kwon, H.-J. & Riley, B. B. Mesendodermal signals required for otic induction: Bmp-antagonists cooperate with Fgf and can facilitate formation of ectopic otic tissue. *Dev. Dynam.* **238**, 1582–1594 (2009).
69. Kwon, H.-J., Bhat, N., Sweet, E. M., Cornell, R. A. & Riley, B. B. Identification of early requirements for preplacodal ectoderm and sensory organ development. *PloS Genet.* **6**, e1001133–e1001133 (2010).
70. Ohyama, T. et al. BMP signaling is necessary for patterning the sensory and nonsensory regions of the developing mammalian cochlea. *J. Neurosci.* **30**, 15044–15051 (2010).
71. Ohyama, T., Mohamed, O. A., Taketo, M. M., Dufort, D. & Groves, A. K. Wnt signals mediate a fate decision between otic placode and epidermis. *Development* **133**, 865–875 (2006).
72. Martins, J.-M. F. et al. Self-organizing 3D human trunk neuromuscular organoids. *Cell Stem Cell* **26**, 172–186.e6 (2020).
73. Kim, J. et al. Human assembloid model of the ascending neural sensory pathway. *Nature* https://doi.org/10.1038/s41586-025-08808-3 (2025).
74. Andersen, J. et al. Generation of functional human 3D cortico-motor assembloids. *Cell* **183**, 1913–1929.e26 (2020).
75. Shearer, A. E. et al. Genetic hearing loss overview. *GeneReviews* [Internet] https://www.ncbi.nlm.nih.gov/books/NBK1434/ (updated 3 April 2025).
76. Williams, D. S. Usher syndrome: animal models, retinal function of Usher proteins, and prospects for gene therapy. *Vis. Res.* **48**, 433–441 (2007).
77. Robertson, N. G. et al. Inner ear localization of mRNA and protein products of COCH, mutated in the sensorineural deafness and vestibular disorder, DFNA9. *Hum. Mol. Genet.* **10**, 2493–2500 (2001).
78. Fukunaga, I. et al. In vitro models of *GJB2*-related hearing loss recapitulate Ca^{2+} transients via a gap junction characteristic of developing cochlea. *Stem Cell Rep.* **7**, 1023–1036 (2016).
79. Fukunaga, I. et al. Modeling gap junction beta 2 gene-related deafness with human iPSC. *Hum. Mol. Genet.* **30**, 1429–1442 (2021).
80. Liu, X.-P., Koehler, K. R., Mikosz, A. M., Hashino, E. & Holt, J. R. Functional development of mechanosensitive hair cells in stem cell-derived organoids parallels native vestibular hair cells. *Nat. Commun.* **7**, 11508 (2016).
81. Azizgolshani, H. et al. High-throughput organ-on-chip platform with integrated programmable fluid flow and real-time sensing for complex tissue models in drug development workflows. *Lab Chip* **21**, 1454–1474 (2021).
82. Shaughnessey, E. M. et al. Evaluation of rapid transepithelial electrical resistance (TEER) measurement as a metric of kidney toxicity in a high-throughput microfluidic culture system. *Sci. Rep.* **12**, 13182 (2022).
83. Novoa, J. J. et al. Good Manufacturing Practice—compliant human induced pluripotent stem cells: from bench to putative clinical products. *Cytotherapy* **26**, 556–566 (2024).
84. Pantazis, C. B. et al. A reference human induced pluripotent stem cell line for large-scale collaborative studies. *Cell Stem Cell* **29**, 1685–1702.e22 (2022).
85. Gopee, N. H. et al. A prenatal skin atlas reveals immune regulation of human skin morphogenesis. *Nature* https://doi.org/10.1038/s41586-024-08002-x (2024).
86. Albanese, A. et al. Multiscale 3D phenotyping of human cerebral organoids. *Sci. Rep.* **10**, 21487 (2020).
87. Park, Y.-G. et al. Protection of tissue physicochemical properties using polyfunctional crosslinkers. *Nat. Biotechnol.* **37**, 73–83 (2019).
88. Lovell-Badge, R. et al. ISSCR guidelines for stem cell research and clinical translation: the 2021 update. *Stem Cell Rep.* **16**, 1398–1408 (2021).

Acknowledgements

K.R.K. is supported by National Institute of Health grants (grant nos R01AR075018, R01DC017461 and R03DC015624) and a Department of Defense grant (grant no. W81XWH211810). W.H.v.d.V. is supported by the Novo Nordisk Foundation (grant no. NNF21CC0073729). C.N.-L. is supported by the National Science Foundation Graduate Research Fellowship Program (grant no. 1000314811) and the National Institute of Deafness and Communication Disorders Ruth L. Kirschstein Predoctoral Fellowship (F31) (grant no. 1F31DC022152-01). M.R.S. is supported by a National Institute of Health grant (grant no. F30DC018715). We thank all the members of the Koehler Lab for their critical insights while preparing this manuscript. We thank C. Moncada-Reid for assisting with the testing of the SHIELD method. Notably, J. Nie, E. Longworth-Mills and E. Hashino were instrumental in the development of this methodology. We especially thank M. Roccio and her team for their insights on performing external replication of the method presented here. We thank all our other collaborators past and present who have assisted us in our evaluation of the inner ear organoid methodology. Fig. 2 was prepared, in part, with resources available from Biorender.

Author contributions

W.H.v.d.V., C.N.-L., J.Z., J.L. and K.R.K. conceived the study and wrote the manuscript. W.H.v.d.V., C.N.-L., J.Z., C.P., J.J., K.Y.G., M.R.S. and J.L. collected and analyzed data. W.H.v.d.V., C.N.-L., J.J., J.L. and K.R.K. contributed to figure making. All authors contributed to the initial manuscript and manuscript editing. J.L. and K.R.K. supervised. All authors read and approved the final manuscript.

Competing interests

K.R.K. and J.L. are inventors on patents relating to the inner ear and skin organoid technology discussed in this article. K.R.K. is a consultant to STEMCELL Technologies, which has licensed the IEO technology.

Additional information

Extended data is available for this paper at https://doi.org/10.1038/s41596-025-01191-3.

Supplementary information The online version contains supplementary material available at https://doi.org/10.1038/s41596-025-01191-3.

Correspondence and requests for materials should be addressed to Jiyoon Lee or Karl R. Koehler.

Peer review information *Nature Protocols* thanks Robert Duncan and Wenyan Li for their contribution to the peer review of this work.

[1]Department of Otolaryngology, Boston Children's Hospital, Boston, MA, USA. [2]F.M. Kirby Neurobiology Center, Boston Children's Hospital, Boston, MA, USA. [3]Department of Otolaryngology-Head and Neck Surgery, Harvard Medical School, Boston, MA, USA. [4]OtoBiology Leiden, Department of Otorhinolaryngology and Head & Neck Surgery, Leiden University Medical Center, Leiden, the Netherlands. [5]The Novo Nordisk Foundation Center for Stem Cell Medicine (reNEW), Leiden University Medical Center, Leiden, the Netherlands. [6]Department of Otolaryngology—Head and Neck Surgery, Indiana University School of Medicine, Indianapolis, IN, USA. [7]Medical Neuroscience Graduate Program, Indiana University School of Medicine, Indianapolis, IN, USA. [8]Department of Plastic and Oral Surgery, Boston Children's Hospital, Boston, MA, USA. [9]These authors contributed equally: Wouter H. van der Valk, Carl Nist-Lund, Jingyuan Zhang.

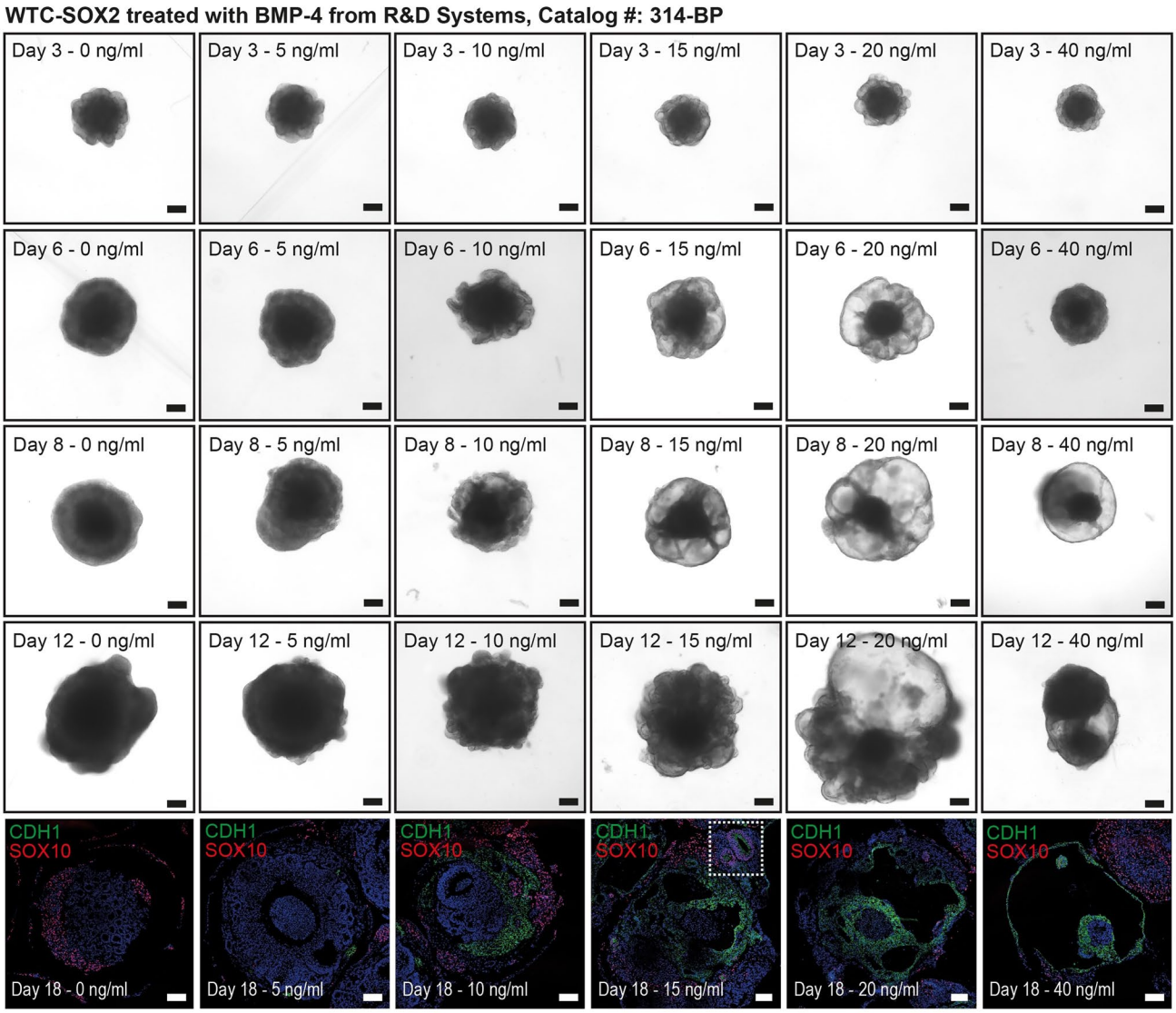

Extended Data Fig. 1 | Dose-dependent effects of BMP4 on organoid development using WTC-SOX2 cells treated with BMP4 from R&D Systems (Catalog #: 314-BP). Brightfield images of organoids at various BMP4 concentrations (0 - 40 ng/mL) on Days 3, 6, 8, and 12. BMP4 from this vendor required a higher concentration for optimal organoid development compared to prior experiments with different BMP4 from other vendors (notably, PeproTech). IHC images of Day 18 organoids (bottom panels) show staining for ECAD (green) and SOX10 (red) across the tested BMP4 concentrations (0 - 40 ng/mL). A Day 18 organoid treated with 15 ng/mL BMP4 shows otic vesicles (highlighted with a white dotted-box). Scale bars, 200 µm (brightfield), 100 µm (IHC data).

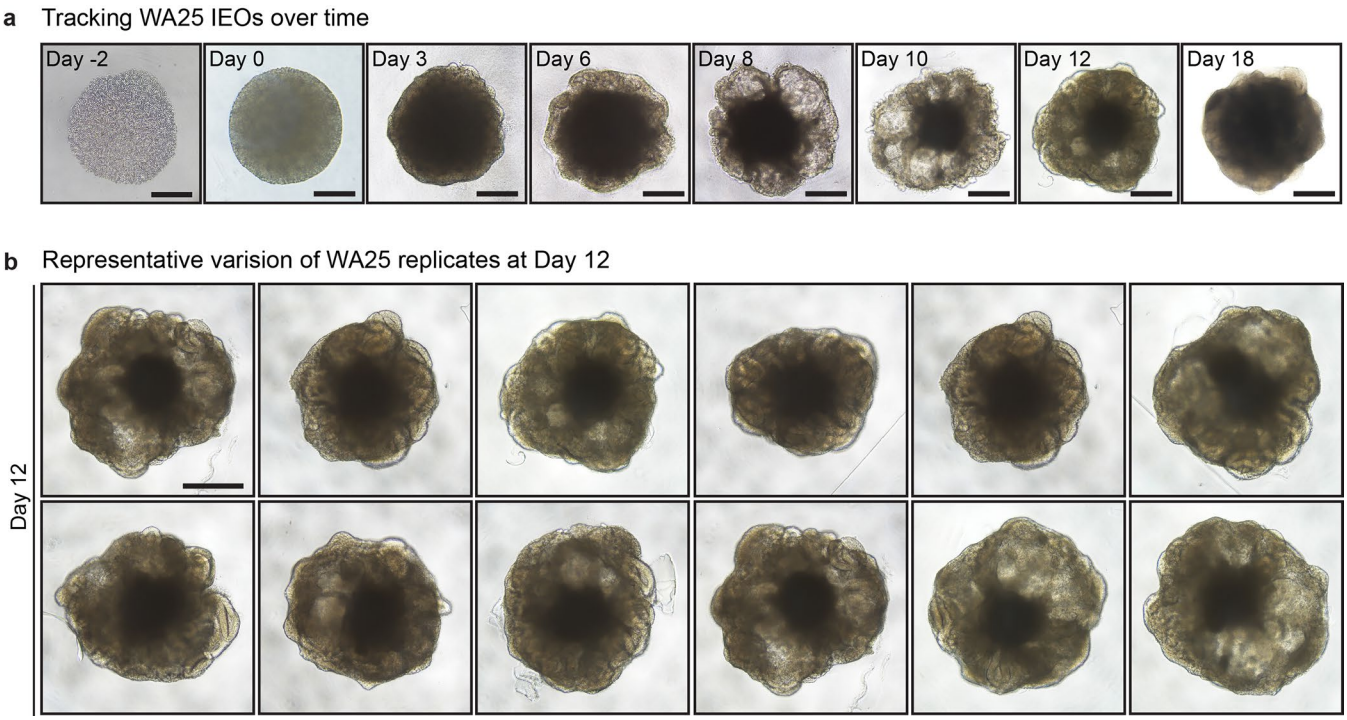

Extended Data Fig. 2 | Brightfield imaging of WA25 cell aggregates over time. (**a**) Representative brightfield images of organoid development over time, derived from WA25 cells treated with 0.5 ng/mL BMP4 on day 0. Images were taken on Day -2, Day 0, and on subsequent days up to Day 18. By Day 12, organoids exhibit a well-expanded, flowery fringe of OEPD epithelium, which is critical for assessing the quality of IEO differentiation. The morphology may vary across different cell lines[29]. (**b**) Brightfield images of organoids on Day 12 representing biological replicates and inter-organoid variability within a single differentiation experiment as those shown in (**a**). Scale bars, 500 µm (a-D-2), 250 µm (**a**-other panels, **b**).